Master's thesis

NTNU
Norwegian University of Science and Technology
Faculty of Engineering
Department of Civil and Environmental Engineering

Raj Kumar KC

Experimental study into the overtopping and breaching of rockfill dams with erosion protection

Master's thesis in Hydropower Development
Supervisor: Fjóla Guðrún Sigtryggsdóttir
Co-supervisor: Geir Helge Kiplesund, Dr. Théo Dezert
June 2022

NTNU
Kunnskap for en bedre verden

Raj Kumar KC

Experimental study into the overtopping and breaching of rockfill dams with erosion protection

Master's thesis in Hydropower Development
Supervisor: Fjóla Guðrún Sigtryggsdóttir
Co-supervisor: Geir Helge Kiplesund, Dr. Théo Dezert
June 2022

Norwegian University of Science and Technology
Faculty of Engineering
Department of Civil and Environmental Engineering

NTNU
Norwegian University of
Science and Technology

NTNU

M.Sc. THESIS ASSIGNMENT

Candidate: Raj Kumar Kc

Title: Experimental study into the overtopping and breaching of rockfill dams with erosion protection.

1. Background

Embankment dams are vulnerable to excess through-flow as well as overtopping, since the dam structure is mainly composed of pervious and erodible materials. The erosion process that initiates in these cases may ultimately lead to breaching of the dam. This process as well as the breach opening are of importance for estimating flooding of the downstream area and mapping of this for flood hazard mitigation. This information influences consequence classification of the dam and consequent dam design requirements.

In Norway embankment dams are typically earth-rockfill dams with erosion protection comprising placed riprap on the upstream and downstream slope and at the crest. The breaching mechanism of these embankment dam types has not been investigated to the fullest. The downstream shoulder of such dams has been studied in recent projects for throughflow and overtopping characteristics, but the effect of the erosion protection on the breaching process of a full dam section needs to be investigated further.

The current practice is to use breaching parameters that are derived without consideration of embankment dam type and material. Albeit expressions that considers simple categorization of the dam type and erodibility of the fill material, exist for the breaching parameters, these have not been used in practice in Norway. Furthermore, it is uncertain how well these expressions capture the effect of the different dam types and different material properties on the breaching parameters. Thus, it is of interest to investigate in more detail the breaching mechanism of rockfill dams, also those that have erosion protection on the downstream slope. This is important for a more reliable consequence classification of typical rockfill dams and also for calculating the flood inundation area in case of a dam breach.

It is against the above background that physical model tests are planned in relation to the project WP1.2 on Dam construction and safety within the research center HydroCen https://www.ntnu.edu/hydrocen/embankment-dam-safety . The tests carried out in this master project are a part of this project and will focus on rockfill dams with a central core and erosion protection comprising riprap on the dam slopes and crest. The model dam shoulders will comprise of well graded rockfill material. This master thesis work will be a step on the way to understand the breaching development of a typical Norwegian rockfill dam designed according to the current dam safety regulations and guidelines.

2. Work description

The thesis will be composed of several tasks related to assessing relevant literature, preparing and running an experimental study on a physical model in the Hydraulic Laboratory at NTNU, and analysing the collected data as well as the observed behaviour. The objectives of the study is: (1) To create experimental data on the breaching of rockfill dams; (2) To investigate the effect of erosion protection

on the downstream slope on the breach process. (3) To use Particle Image Velocity method to analyze the failure mechanism of the riprap and identify the failure initiation. (4) To compare results from the experimental tests on the physical model to calculated breaching parameters from selected parametric breach models.

The specific tasks are detailed as follows.

1. Carrying out a literature review into the state of the art within the discipline of breaching of embankment dams and the Particle Image Velocity (PIV) method.
2. Plan and carry out model tests on a physical model in the hydraulic laboratory of the department. The model setups will include: a rockfill dam with a central core and erosion protection on the slopes and at the crest. The dams will be built along with a fellow student or a research assistance. In return the student will help his fellow on other similar tests. Additionally, the student will have access to result from related tests carried out in the project by others. The test will be carried out under the supervision of Geir Helge Kiplesund and Dr. Théo Dezert.
3. Qualitative and quantitative analysis of the breaching process.
4. Present and discuss pore water pressure measurements.
5. Use waterlevel measurements and inflow discharge to calculate the outflow discharge.
6. Use of PIV to further describe the failure mechanism and find the location within the dam where the failure initiates.
7. Discuss limitation of the setup.
8. Compare results with earlier research on failure in riprap without supporting fill (e.g. Priska Hiller, Ganesh H.R. Ravindra)
9. Draw conclusion from the work and propose further studies.

3. Supervision

Professor Fjola Gudrun Sigtryggsdottir will be the supervisor of the thesis work along with the PhD candidate Geir Helge Kiplesund and Dr. Théo Dezert.
Discussion with, and input from colleagues and other researchers or engineering staff at NTNU, SINTEF, power companies or consultants is highly recommended. Significant inputs from others shall, however, be referenced to in a convenient manner.
The research and engineering work carried out by the candidate in connection with this thesis shall remain within an educational context. The candidate and the supervisors are therefore free to introduce assumptions and limitations, which may be considered unrealistic or inappropriate in a contract research or a professional engineering context.

4. Report format and submission

The report should be written with a text editing software. Figures, tables and photos shall be of high quality. The report format shall be in the style of scientific reports and must contain a summary, a table of content, and a list of references and information about other relevant sources.
The report shall be submitted electronically in Inspera Assessment (IA) along with a summary. The summary shall not exceed 450 words. Supplementary working files such as spreadsheets, numerical

models, program scripts, figures and pictures shall be uploaded to Inspera Assessment (IA) as applies or submitted to the supervisor.
The candidate shall present the work at an MSc seminar. The presentation shall be given with the use of powerpoint or similar presentation tools. The data and format for the MSc. seminar will be announced during the semester. The Master's thesis should be submitted by the end of the spring semester as specified by the Department of Civil and Environmental Engineering.

_____

Fjóla Guðrún Sigtryggsdóttir
Professor
Department of Civil and Environmental Engineering, NTNU

Abstract

Embankment dams are mainly made of erodible and pervious materials and are at risk from overtopping and piping, the erosion process that initiates may ultimately lead to the dam breaching. Estimating the flood and mapping the downstream area of the dam is essential to minimize the risk in the future due to the dam's collapse. This flood calculation requires understanding the breaching mechanism and breach opening parameters. In Norway, earthfill dams are protected by placed ripraps on the upstream, downstream, and crest. Thus, this thesis aims at adding some information to the understanding of the breaching mechanism and process,breaching rate, examining the breaching parameters, and calculating outflow peak discharge during the breaching event. In this thesis, experiments were carried out on a scale of 1:10 on dam models with placed riprap, single-layer dumped riprap, and double-layer dumped riprap each. Through experimentation and later analysis of these experiments, it is found that both placed and dumped riprap failure starts from just downstream edge of the crest in overtopping during breaching. Breach parameters calculated from available empirical relations significantly differ from the data obtained from the experiment. The data plot revealed that we could relate inflow breach discharge and outflow peak discharge with a linear equation. During the PIV analysis, it was observed that the failure between two dumped riprap was similar while observation with placed riprap was different. Through PIV analysis, it was also found that the breach in placed riprap occurs abruptly, and failure in both dumped and placed riprap starts just downstream section of the dam.

Preface

The author of this thesis is from Nepal; most of the hydroelectric projects in Nepal are run-of-river types of projects producing surplus energy during the rainy season; however a power deficit during the winter season. Nepal faces frequent earthquake problems. These problems can be addressed by constructing the Rockfill dam, as it can be built from locally available material and have a minimal effect due to earthquakes. These rockfill dams have breaching problems on overtopping and piping action. This exciting fact made the author do a Master's Thesis on Rockfill dam for the partial fulfillment of a two-year MSc. program in Hydropower Development at NTNU. The author was involved in constructing and testing eight embankment dams in the hydraulic laboratory at the Department of Civil and Environmental Engineering. He worked as a Research Assistant in the construction of Rockfill dams in his Second semester for Ph.D. candidate Geir Helge Kiplesund. The author and his classmate Saroj Sapkota helped each other to construct rockfill dams and homogenous dams for their master thesis from December 2021 to late January 2022. Only models with riprap are used in this thesis for analysis. All these tests are constructed under the guidance of the main supervisor, Fjóla Guðrún Sigtryggsdóttir, and Co-supervisors: Geir Helge Kiplesund, Dr. Théo Dezert.

Acknowledgements

First of all, I would like to thank my primary supervisor, Associate Professor Fjóla G. Sigtryggsdóttir, for her proper guidance during this thesis. She has given me the flexibility in the study direction I want and constantly encouraged me to follow up on my thesis progress.

I am delighted to have Geir Helge Kiplesund as my co-supervisor for this master thesis. He helped me with many things, such as in the laboratory, data analysis, and also provided an idea of how to present the result using QGIS.

I want to thank my classmate Saroj Sapkota for helping me during the construction phase, making my time available even on the weekends, and agreeing to work sometimes long hours. He is my friend from back in Nepal and has 8-9 years of friendship thanks for cracking lots of jokes in the lab during construction.

I want to thank Dr. Théo Dezert for helping me in the construction of one dam and Mr. Geir Tesaker and Mr. Thai Mai for providing technical and logistical support.

Contents

Figures

Tables

Chapter 1

Introduction

A dam is a barrier built across a river, a stream, or an estuary that retains the flow of water. Dams were constructed in ancient times for a single purpose: water supply or irrigation. With the development of civilizations, there was a greater need for water supply, irrigation, flood control, navigation, water quality, sediment control, and energy. Therefore, dams are built for specific purposes such as water supply, flood control, irrigation, navigation, sedimentation control, and hydropower. The dam is the cornerstone in developing and managing water resources in a river basin. In developing countries, the multipurpose dam is essential because the population receives domestic and economic benefits from a single investment (ICOLD 2022).

Water demand is continuously growing over the world. Apart from air and land, there is no life on Earth without water, which is our most crucial resource. The quantity of water extracted from freshwater resources has risen by a factor of 35 during the last three centuries, while the global population has expanded by a factor of 8. With the world's growing population, global water consumption is likely to climb by another 2-3 percent yearly in the following decades. On the other hand, freshwater resources are scarce and unevenly distributed. This problem can be addressed by the construction of the dam (ICOLD 2022).

"A large dam" is defined by the International Commission on Large Dams (ICOLD) as a dam that is 15 m or greater from foundation to crest, or a dam between 5 and 15 m high that impounds a volume greater than 3 million cubic meters (MCM) (ICOLD 2011). There are different types of dams available such as Concrete Gravity Dam, Arch Dam, Embankment dams, and Buttress dams, and the selection of the dam is made based on location, construction material availability, and construction cost. This thesis talks about Rockfill Embankment Dams.

1.1 Embankment dams

Any dam constructed of excavated natural materials or waste materials(ICOLD definition). Embankment dams can be homogeneous, i.e., constructed mainly of a single kind of material. (however, with riprap and toe drain) and Zoned, i.e., Constructed of more than one material. Usually with a central impervious core of clay or moraine, abutted with filters and supporting. Here are some reasons for the selection of an embankment dam. It is suitable in wide valleys as well as relatively steep-sided gorges and can be used in a variety of foundation conditions, from competent rock to soft and compressible soils, as well as reasonably pervious soil or rock formations. A well-built embankment dam can safely accept a significant amount of deformation and settlement while minimizing the danger of major cracking and failure

1.2 Rockfill dams

Embankment dams come in two different types earth fill and rockfill dams. Depending on the predominant fill material, a dam-type is defined as earth fill if it contains 50 % or more of clay, silt, sand, or gravel, whereas dams that contain 50 % or more blasted rock is defined as rockfill Kjærnsli et al. (1992).

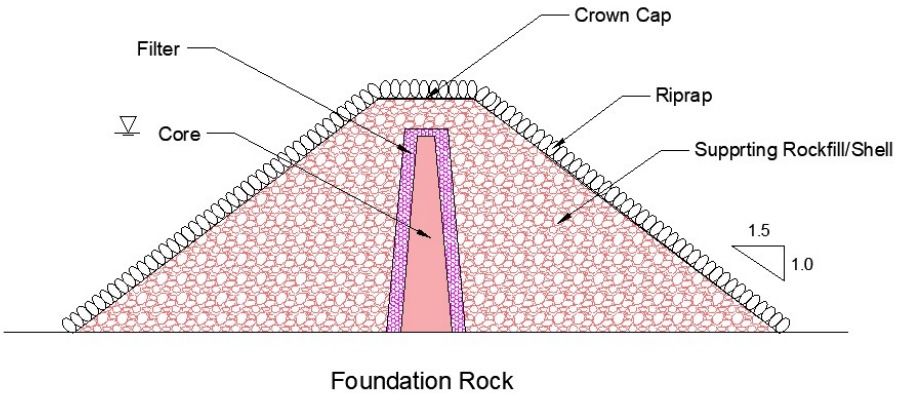

Figure 1.1: Sketch of rockfill dams with a central core and erosion protection on the dam slopes.

The core is the impervious body of the dam, which restricts the flow through the dam structure. The core is usually made of a moraine, glacial till, clay, silt, asphalt concrete, and bitumen. Filter helps to minimize the internal erosion of finely graded material from the core. It also acts to minimize the pore pressure

and heal the minor cracks in the core. This filter is generally made of sandy gravel. The primary function of Supporting Rockfill/shell material is to provide support to the core and to stabilize the whole dam structure. It usually consists of blasted rocks. The riprap is placed on the upstream slope. In Norway, riprap is also placed on the downstream slope and the top of the dam. The main function of riprap is to protect against erosion on the downstream side. In the upstream side, riprap protects from wave action and forces that develop during changes in reservoir water level. This riprap can be both dumped and placed. This riprap consists of large boulders. A crown cap is made of a large boulder or gravel and serves as a protective layer to the dam.

1.3 Scope and objective

The Scope of this thesis is to do an experimental study into the overtopping and breaching of rockfill dams with erosion protection, and this is carried out in three main tasks. The first step is to review the literature on the breaching process in embankment dams due to through flow and overtopping. The second step is to perform physical tests on rockfill dams with a central core and investigate the effects of erosion protection on the downstream slope. Lastly breaching process from the experiment is analyzed visually and using the particle image velocity analyses method (Fudaa software).
The thesis aims to answer the following questions by completing the tasks; Qualitative and quantitative analysis of the breaching process, pore water pressure development inside the dam at different discharge, water level measurements, and inflow discharge to calculate the outflow discharge, using the PIV method to describe the failure mechanism further and find the location within the dam where the failure initiates, compare results with earlier research on failure in riprap without supporting fill.

Chapter 2

Background

This chapter is about major failure mechanisms in embankment dams, such as overtopping, internal erosion, and piping. One common measure for such failure is placing riprap on the upstream and downstream sides of the dam, and these ripraps are available in two types: placed and dumped. We need to designthe proper shape, size, and volume of riprap, which can provide stability to the dam. Breaching of the dam during failure can be modeled in three ways: empirical, semi-physical, and physical. For proper modeling, we need different breaching parameters such as geometric and hydrographic.

In some cases breaching process is so abrupt it's hard to find the breach initiation point and how it progress. This problem can be solved with the help of the image analysis from video footage and the particle image velocimetry method(PIV analysis). The software used in this thesis for such analysis is Fudaa LSPIV analysis, which is described in this chapter.

2.1 Dam failure

The primary dam failure modes are Overtopping, Internal erosion(piping), slope instability, and seismic failure.Overtopping(48%) and internal erosion (46%) are the most common modes of embankment dam failure. These two modes can be a tie-up with slope instability. (Fell et al. 2005).

2.1.1 Overtopping

The surface erosion process involves removing material from the dam surface, usually caused by overtopping the dam crest and crossing the downstream slope. This material removal can lead to the instability and failure of the dam. Inadequate capacity of the spillway to pass flood discharge, malfunction of gates, and other outlets may lead to overtopping. An illustration of overtopping is shown in figure 2.1 below.

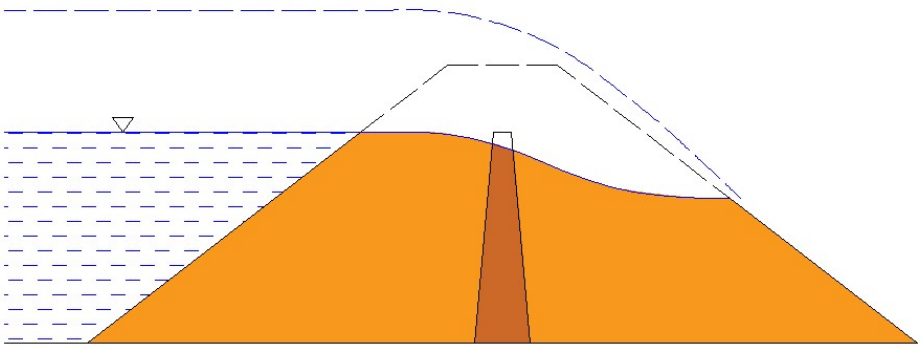

Figure 2.1: Overtopping in Embankment Dam.

2.1.2 Internal Erosion and Piping

Internal erosion occurs when the water seeps through the dam and carries the soil particles away from the dam's filters, embankments, drains, foundations, or abutments. If the seepage through the downstream side of the dam approaches the reservoir, then catastrophic dam failure can occur. The process of internal erosion can be broadly divided into four phases initiation of erosion, continuation of erosion, progression to form a pipe and initiation of a breach. (Fell et al. 2005)

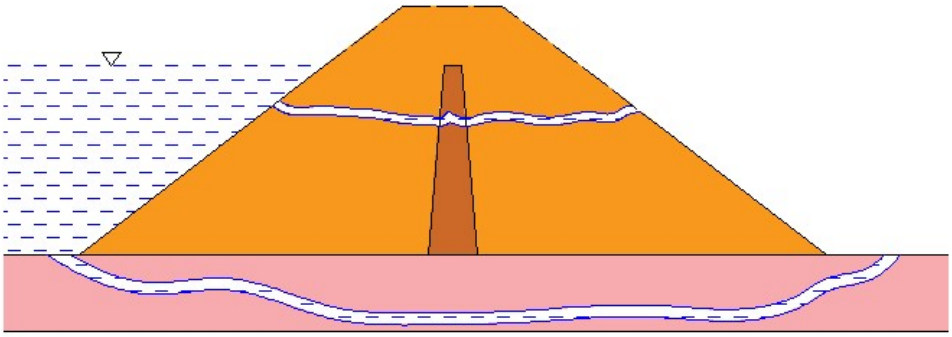

Figure 2.2: Internal Erosion and Piping in Embankment Dam

When there is some crack or weakness in the core, it causes the seepage flow on the dam's downstream side. This pore water pressure decreases the effective stress of dam material and increases the destabilizing forces. The leaked water from the core exits a specific point on the downstream side of the dam, creating a flow path, fine material inflow path starts to erode, forming a channel. Expansion of the channel starts and approaches towards the upstream side of the dam and to the reservoir. This progression of channels creates a bigger size of voids and

settlements, leading to the collapse of a dam.

2.2 Protection Measures

Boulder riprap is placed on the upstream and downstream sides of the dams to protect the dam from overtopping and internal erosion. On the upstream side of the dam, riprap protects from wave action, ice, and change in water level. On the dam's downstream side, riprap protects from surface erosion due to through flow and overflow conditions. However, from an experiment conducted during this thesis at NTNU lab, it is found that riprap can only handle overtopping for a specific range of overtopping discharge, and the period beyond that dam starts to breach. Riprap is divided into two categories based on construction methodology dumped and placed riprap. Dumped riprap is placed randomly while placed riprap are arranged in a specific interlocking pattern. The experiment found that placed riprap is more resilient to erosion protection than dumped riprap. Dumped riprap is more economical and less time-consuming to construct compared to placed riprap (Ravindra 2018).

During the 1960s and 70s, many dams were constructed, and the size and volume increased. Different efforts were applied for the optimization of the dam and to get durable structures with an economical design. Some of the strategies are the construction of spillways to pass floods and riprap on the downstream and upstream sides to combat overtopping and internal erosion. Construction of spillway helps to minimize the freeboard height, hence economical (Hiller 2017).

2.2.1 Riprap Parameters

The interaction between the riprap and hydraulic force determines the stability of the riprap. The parameters can be divided into riprap, hydraulic and geometric boundary conditions. Slope (Z), an extension of the slope covered with riprap exposed to overtopping Ls, and the width of the dam (B) are the characteristics of Geometric boundary conditions (Hiller 2017).

Riprap stones are characterized by size, which can be expressed through the diameter, volume, or mass. Volume and mass parameters are related to each other.

$$V_s = C_f d^3 = C_f m_s * \rho_s^{-}1 \tag{2.1}$$

where: V_s = Volume
m_s = mass
d = diameer
C_f = form factor
C = stone density

C_f factor varies between 0.4 for schistose rock and 0.8 for cubical (NVE 2012)

The diameter can be expressed as equivalent sphere diameter, which means the nominal diameter d of riprap stone has the same volume as the corresponding sphere with diameter d_s. The nominal diameter of the stone is given as (Bunte 2001).

$$D_n = (abc)^{1/3} \tag{2.2}$$

where: a = Longest axes
b = Intermediate
c = Shortest axes

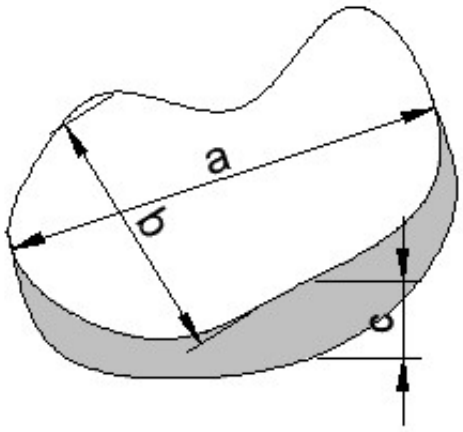

Figure 2.3: Stone with three different axes

Particle size distribution curve is used for grading of stones; the index i and d_i give the percentage by mass which is finer than d_i. The common coefficient of uniformity is given as

$$C_u = d_{60}/d_{10} \tag{2.3}$$

where: d_{60} = Particle finer than 60%
d_{10} = Particle finer than 10%

Abt and Ullaman (2008) found that round stone needs to be approximately 40% larger in size compare to angular stones to withstand similar kind of hydraulic

forces. The parameters such as angle of repose, aspect ratio and weathering resistance can be added to describe stone material in more detail.

The orientation of the stone in placed riprap can be described with angle β between the surface and longest axis of the stone, which is shown in figure 2.4 below.

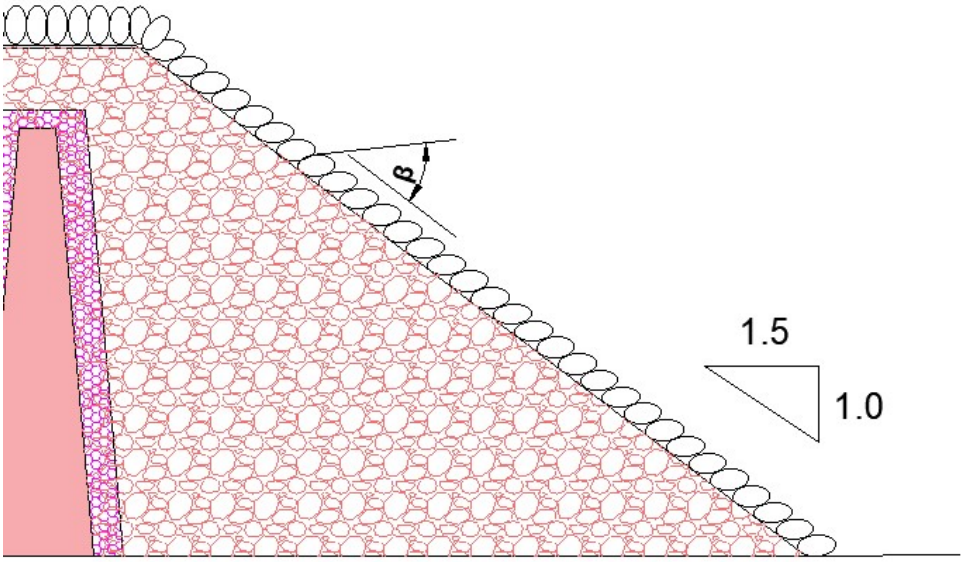

Figure 2.4: Downstream slope and the inclination β of the riprap stones

There has not been found the common way to describe quality of placed and dumped riprap, however packing density factor seems to be a good indicator.The packing factor given by (Olivier 1967).

$$P_c = 1/N d_s^2 \tag{2.4}$$

where: P_c = Packing factor
N = number of stones per m^2
d_s = Nominal diameter

Low packing factor gives high density and vice versa; during the test conducted during this thesis at NTNU Lab, it was found that the placed riprap has a lower P_c value compared to dumped riprap.

Regarding the hydraulic properties, flow velocity (v) is the key parameter to describe hydraulic forces such as drag,lift and shear force. Flow over riprap is driven by the gravity and characterized by froude number (F), Reynold's number(R) and Weber number (W) (Hiller 2017).

$$F = v/\sqrt{gh} \tag{2.5}$$

$$R = vh/\nu \tag{2.6}$$

$$W = \rho_w h v^2 / \sigma \tag{2.7}$$

where: v = Flow velocity
h = Water level
ν = Kinematic viscosity
g = acceleration due to gravity
ρ_w = density of water
σ = Surface tension

Reynold's number can be neglected if the flow in the model is turbulent, Weber number is relevant to describe the transport of air. For high-speed air-water flow scaled with Froude similitude, Pfister and Chanson (2012) recommend $W^{0.5} >$ 140 or R $>$ 2 to 3x10^5 to prevent significant scale effects.

Hiller (2017) used Froude number combine with relative submergence to the stone-related Froude number with discharge per unit width $q = vh$. Stone-related Froude number helps to compare the test result at different scales. It is difficult to find the v and h in supercritical flow conditions as depth and velocity constantly change whereas their product remains constant until the geometry changes. Stone related Froude number is given as

$$F_s = q / \sqrt{g d^3} \tag{2.8}$$

2.2.2 Failure mechanism in Riprap

The riprap which is exposed to overtopping can be characterized by different failure mechanisms. The failure mechanism can be a removal of a single layer of stone, sliding of the protection layer, and disruption of the protection layer, as shown in figure 2.5 below (Siebel 2007).

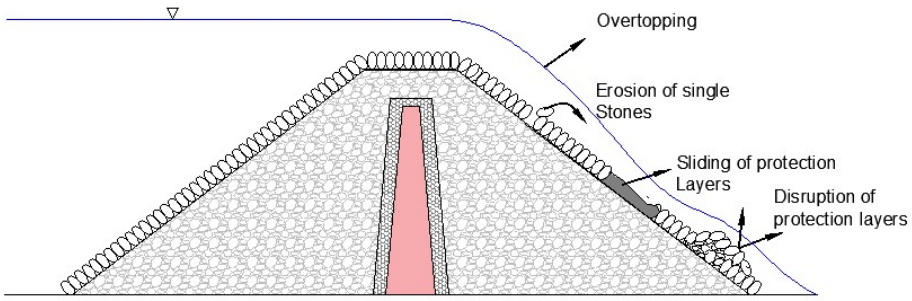

Figure 2.5: Failure mechanism in riprap exposed to overtopping

failure in dumped riprap failure occurs when there is sufficient erosion leading to exposure of filter material, while in placed riprap there is an interlocking pattern.

Interlocking pattern makes placed riprap to bear some more loads and do not fail quickly, even there is the removal of some stones leading to expose the filter materials. (Ravindra 2018).

2.2.3 Load Resolution at Riprap

When the boulder riprap is at rest, different forces act on it, the mass(m) multiplied by the acceleration due to gravity (g) gives the weight of the riprap, which acts downwards in the direction of gravity. The inclination angle θ is the riprap slope. The weight (W) can now be resolved into two different components $Wsin\theta$ acts in the direction of the slope and $Wcos\theta$ acts normal to the slope, F_L is the uplift force. $Wsin\theta$ tries to take the riprap in motion while $\mu(Wcos\theta\text{-}F_L)$ acts in opposite direction to stabilize the riprap. During the time of overtopping the extra force, F acts in the direction of $Wsin\theta$, which is shown in figure 2.6 below.

$$\mu(Wcos\theta - F_L) > Wsin\theta + F \quad (No \;\; Slide) \tag{2.9}$$

$$\mu(Wcos\theta - F_L) < Wsin\theta + F \quad (Slide \;\; Starts) \tag{2.10}$$

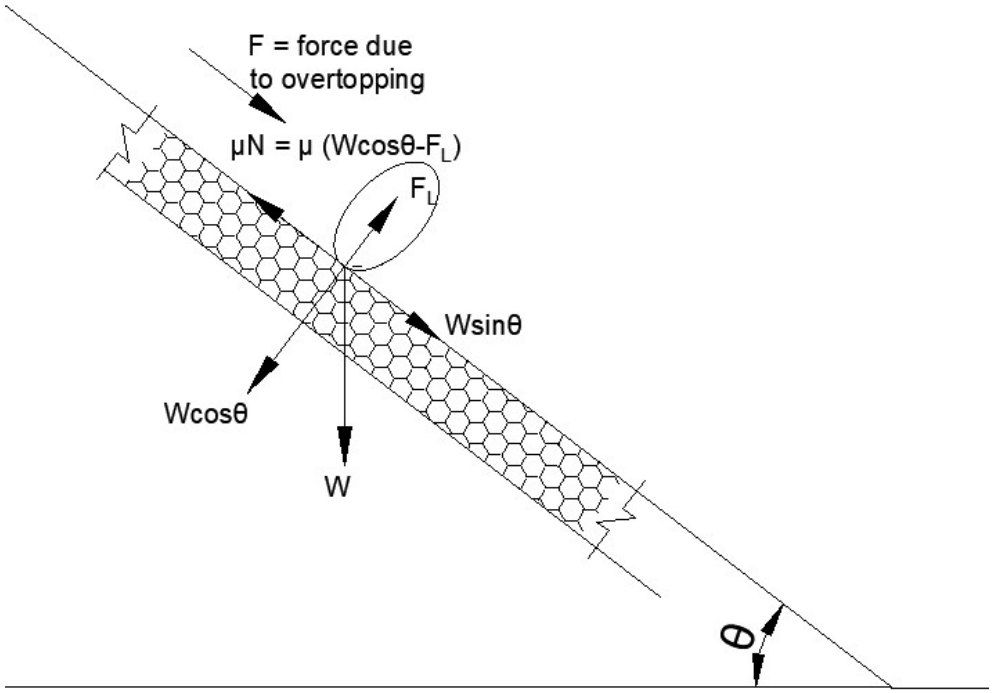

Figure 2.6: Load resolution at boulder Riprap

2.3 Breach Parameters

Dam breach parameters can be divided into two groups Geometric and Hydrographic Parameters. Dam breach often has a trapezoid shape, with the geometric parameters of breach depth (H_b), breach top width (B_t), average breach width (B_{ave}), breach bottom width (B_b) and breach side slope factor (Z) as shown in figure 2.7 below. Any combination of three of five parameters determines the breach shape and size (Xu and Zhang 2009)

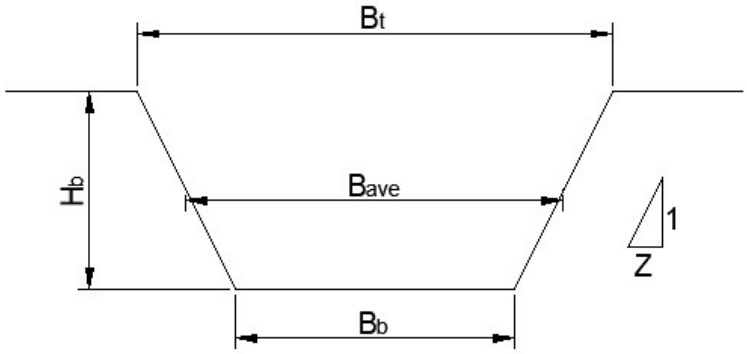

Figure 2.7: Geometric Parameters of Dam Breach

Hydrographic Parameters include peak outflow rate (Q_p), and failure time (t_f). After the onset of breaching, the outflow through the breach increases until it reaches a peak (Q_p), and then decreases until there is no water in the reservoir or the breaching process ceases to develop. Failure time (t_f) is defined as the period from the inception to the completion of the breaching process (Xu and Zhang 2009)

2.4 Breach Models

Different models are used to find the breaching process in an embankment dam based on their complexity. For the past 50 years, engineers and researchers have been trying to develop improved models. Different types of breaching models are empirical models, Semi physically-based (analytical and parametric models), and Physically-based models (Morris 2009).

2.4.1 Empirical models

Empirical models are based on data collected from previous dam breach events. Different breach parameters such as Peak discharge, dam breach width, height, etc. are determined from empirical equations (Morris 2009). The main benefit of using such an equation is its simplicity, no need for a computer program. This simplicity is also causing its main weakness leading to uncertainty within predictions. The other disadvantage of this model is it only gives discrete values instead of the process involved to find the value, for example, peak discharge instead of the whole hydrograph, breach width instead of time-varying width.

Xu and Zhang (2009) studied through 182 historic dam failures had developed empirical equations which consider the physical condition to determine the embankment breach parameters. More than 50 % of dams were 15 m or higher, The model they derived distinguishes the failure caused by overtopping or piping and also takes into account of erodobility factors low, medium, or high. This is not studied in most of the other studies. Their paper presents the equation for determining the top width, average width, breach peak discharge, and failure time.

$$\frac{B_t}{h_b} = 1.062\left(\frac{h_d}{h_r}\right)^{0.092}\left(\frac{V_w^{1/3}}{h_w}\right)^{0.508} e^{B_2} \tag{2.11}$$

Where, B_t = Top width(m), h_b = height of breach (m), h_d = Height of the dam (m), V_w = Volume of water stored above breach bottom (m^3), h_w = Height of the water above breach bottom (m), B_2= b_3+b_4+b_5 in which b_3 is 0.061, 0.088 and -0.089 for dams with corewalls,concrete faced dams, and homogeneous/zoned dams, respectively. b4 is 0.299 for overtopping and -0.239 for piping, b5 is 0.411, -0.062, and -0.289 for high, medium, and low dam erodibility, respectively finally h_r is defined as 15.0 m.

$$\frac{B_{avg}}{h_b} = 0.787\left(\frac{h_d}{h_r}\right)^{0.133}\left(\frac{V_w^{1/3}}{h_w}\right)^{0.652} e^{B_3} \tag{2.12}$$

Where, B_3=b_3+b_4+b_5, in which b_3=0.041, 0.026, and 0.226 for dams with core-walls, concrete faced dams, and homogeneous/ zoned-fill dams, respectively, b_4= 0.149 and 0.389 for overtopping and seepage erosion/piping, respectively, b_5= 0.291, 0.14, and 0.391 for high, medium, and low dam erodibility, respectively.

$$\frac{Q_p}{\sqrt{gV_w^{5/3}}} = 0.175(\frac{h_d}{h_r})^{0.199}(\frac{V_w^{1/3}}{h_w})^{-1.274}e^{B_4} \tag{2.13}$$

where, B_4=b_3+b_4+b_5, in which b_3=0.503, 0.591, and 0.649 for dams with core walls, concrete faced dams, and homogeneous/ zoned-fill dams, respectively, b_4=0.705 and 1.039 for overtopping and seepage erosion/piping, respectively, b_5=0.007,0.375, and 1.362 for high, medium, and low dam erodibility,respectively.

$$\frac{t_f}{t_r} = 0.304(\frac{h_d}{h_r})^{0.707}(\frac{V_w^{1/3}}{h_w})^{1.228}e^{B_5} \tag{2.14}$$

with B_5=b_3+b_4+b_5, in which b_3=0.327, 0.674, and 0.189 for dams with core-walls, concrete faced dams, and homogeneous/zoned-fill dams, respectively, b_4=0.579 and 0.611 for overtopping and seepage erosion/piping, respectively, b_5=1.205,0.564, and 0.579 for high, medium, and low dam erodibility,respectively, t_r is defined as 1 hr.

Froehlich (1995a) revisited his previous studies conducted in 1987 and collected data of 65 more embankment dam failures. This study aimed to estimate the breach parameters such as average width, side slope ratio, and breach failure time.

$$B_{avg} = 0.1803k_0V_w^{0.295}h_b^{0.19} \tag{2.15}$$

Where h_b is the height of the breach. If failure is due to overtopping average breach width is 40 percent larger.

k_0 = 1.4 for overtopping and 1.0 for other failure modes

In figure 2.7 slope ratio can be taken as z = 1.4 for overtopping failure and 0.9 for other types of failure. The failure time given by Froehlich (1995a)

$$t_f = 0.00254(V_w)^{0.53}h_b^{-0.9} \tag{2.16}$$

Froehlich (1995b) studied 22 historical embankment dams and analyzed multiple linear regression equations. All the variables from breach parameters were transferred by logarithmic calculation to get the best linear relation to estimating the peak discharge. The peak discharge equation is given below.

$$Q_p = 0.607(V_w^{0.295} h_w^{1.24}) \tag{2.17}$$

where: Q_p = Peak outflow(m^3/s)
V_w = Volume of water stored above breach invert at the time of failure (m^3)
h_w = Depth of water above breach invert at the time of failure (m)

U.S.Bureau (1988) using the SMPDBK model gives the guidelines for the determination of breach parameters and also failure time. The value determination from US reclamation is not pretty accurate; however, it tends to provide better value than conservative values. It gives value to both earthen dams and non-earth fill dams.

$$B_{avg} = 3h_w(forearthfilldams) \tag{2.18}$$

$$B_{avg} = 2.5h_w(fornonearthfilldams) \tag{2.19}$$

failure time given by U.S.Bureau 1988

$$t_f = 0.011(B_{avg}) \tag{2.20}$$

Peak discharge given by U.S.Bureau 1988

$$Q_p = 19.1(H_w)^{1.85} \tag{2.21}$$

2.4.2 Semi-physically based, analytical and parametric models

In empirical model there is a high level of uncertainty associated with the physical model high level of complexity led authors such as Singh(Singh and Scarlatos 1989) and Walder(Walder and O'Connor 1997) to develop a model which based on a process with simplified assumptions to model the breaching of earth fill dams (Morris 2009).

The assumptions which are usually made in such models

1. A weir equation can adequately present the flow over the embankment
2. Critical flow conditions exist on the embankment crest
3. The breach growth process is time-dependent

The outflow hydrograph from failed embankment dam can be developed based on the above assumptions. Even though these models are simple to find the growth or breach of embankment dams often user requires to provide an erosion rate. The model simply considers the growth pattern to fit these different parameters

to produce a flood hydrograph. Although these parameters can not be found easily and differ significantly from dam to dam. This model is more accurate compared to empirical model.

2.4.3 Physically based models

The physical model can simulate embankment dams' failure based on processes observed during failure such as erosion, flow resign, and instability process. During the last 40 years, period different models have been developed to simulate the failure mechanism; these models may be different based on their complexity, assumptions, and techniques used (Morris 2009).

The advantages of using physically-based models include

- Observed physical processes such as aspects of hydraulics, sediment transport, soil mechanism, and structural behavior are used to simulate the growth breach process.
- without redefining the growth process, a real estimate of the outflow hydrograph and breach process can be predicted.
- In model, uncertainties within the parameters can be included.

The disadvantages of using physically based models include

- Computer programs are required for simulation, the running time may be much longer based on their complexity.
- Currently there are different types of computing programs are available such as 1D, 2D , 3D

2.5 Particle Image Velocity (PIV) Analysis

2.5.1 Why we Need PIV anlaysis

There is often a mismatch between available hydrometric measurements and needs during the study of liquid flow or sediment flow in a river. This led to the development of numerical modeling towards demands for specialized data, with high frequency for various flow conditions. During the flood period, it's difficult to measure the velocity and discharge using a traditional method such as the current meters or flow dilution method due to high velocity and floating debris. Sometimes these flow techniques are not working properly in the unsteady nature of flood flows. Understanding the flowing nature in rivers and labs requires the development of 2D or 3D modeling tools. The alternative way to measure the instantaneous velocity is hydrometry by image sequence analysis. This is applicable to find the surface velocities up to the hectare in a non-intrusive way (Walder and O'Connor 2018).

2.5.2 Principles of the PIV

Image sequence analysis makes it possible to measure the 2D field of velocity on the flow surface with visible tracers, such as solid particles, bubbles or turbulence advected with the flow. This technique was developed from the particle image velocimetry used in the laboratory however this is also used in large scale river hence named it as Large scale PIV (Fujita 1998).

An LSPIV analysis consists of

- recording a sequence of timestamped images of the flow
- a geometric correction of the images to overcome perspective distortion effects (orthorectification)
- calculation displacement of the tracers of the flow through a statistical correlation of the reasons.

In the following cases there is no necessity to seed the flow by adding tracer, flooded river if the water movement is visible in a sequence of images. It is possible to extract velocities nearly in instantaneous 2D field in such cases. When the cross-section of the river is known and assuming the vertical velocity distribution we can calculate the discharge of the river from the LSPIV velocity field.

LSPIV has been used in many rivers with very different scales from low to high floods and to improve calibration curves in normal hydraulic regimes. Review on LSPIV application for different rivers have been proposed by (Muste M 2008). Studying runoff LSPIV has also been proved to be an effective tool. LSPIV has been proven to be an effective tool to study runoff where intrusive instruments cannot be used due to very weak tie rods (Nord G 2009)

2.5.3 Fudaa LSPIV

In this thesis, Fudaa LSPIV software is used to calculate the instantaneous velocity of the particle during breaching time. This software process sequence of flow images to calculate surface velocity fields and flow rate across cross-sections. This method is based on large scale particle image velocimetry (LSPIV) technique with the following steps.

- Source images: import a sequence of images or sample images from a video clip
- Orthorectification: Correct images from perspective distortion and assign a metric size to pixels
- PIV analysis: calculate surface velocities from statistical analysis of tracer movement
- Post-processing: apply filters to the velocity results, calculate the time average, calculate the streamlines

- Discharge: calculate discharge through a bathymetric transect using a velocity correction coefficient

Fudaa-LSPIV is a java interface that calls Fortran for execution. DeltaCAD has been executing and developing Fudaa LSPIV since August 2010. This development is part of free software development for hydraulic applications. Fudaa can run in Windows or Linux operating systems and is available in two languages, French and English. (Walder and O'Connor 2018).

Chapter 3

Method

Construction and test of embankment dam were carried out at NTNU laboratory. The flume was built at the lab before this thesis, and its shape, size, inflow, and outflow mechanism of the inflow pump are described below, eight tests were conducted during the thesis work, but only the models with riprap are used in this thesis for analysis, other tests comprised homogeneous rockfill dams and dams with a central core but no riprap. The material section talks about the grain size distribution of filter and shell materials and riprap size determination. The construction section describes the procedure to prepare the physical dam model from the initial setup to the end. In the testing procedure section, there were 6-9 cameras to capture the failure mechanism and ten pressure sensor pipes to measure the pressure continuously.

3.1 Model setup

The physical model tests were conducted in a flume having the following dimensions 25 m in length, 1 m in breadth, and 2 m in height. This flume has four large glass panes on a testing side to capture the video during the experiment from the left bank side shown in figure 3.1 and figure 3.2. The flow was generated by two pumps having a combined maximum inflow capacity of 0.5 m^3/s. There are several holes in inflow pipes for better distribution of the large incoming volume of water, and his inflow water was collected in a reservoir(9) to prevent turbulent inflow water during the experiment. The aluminium platform (11) was constructed to support the model and to minimize the effect caused by the backwater effect on the downstream side of the dam. This aluminium platform was 0.35 m in height from the bottom of the flume; this was raised in a single vertical step on the upstream side of the dam and smooth slope on the downstream side of the model, stretching approximately 6.5 m in length. The geotextile fabric covered the elevated aluminum surface to prevent the artificial smooth surface, which can cause the unwanted and impractical sliding of material along the bottom surface. The (6) mark indicates the outlet for incoming discharge. On the upstream side, to control the incoming discharge and remove the water collected in 0.35 m vertical step, there was a bypass pipe indicated by the (7) mark. The experiment was captured by the (7) overhead camera indicated by (1) mark and the side camera

indicated by (2) mark.

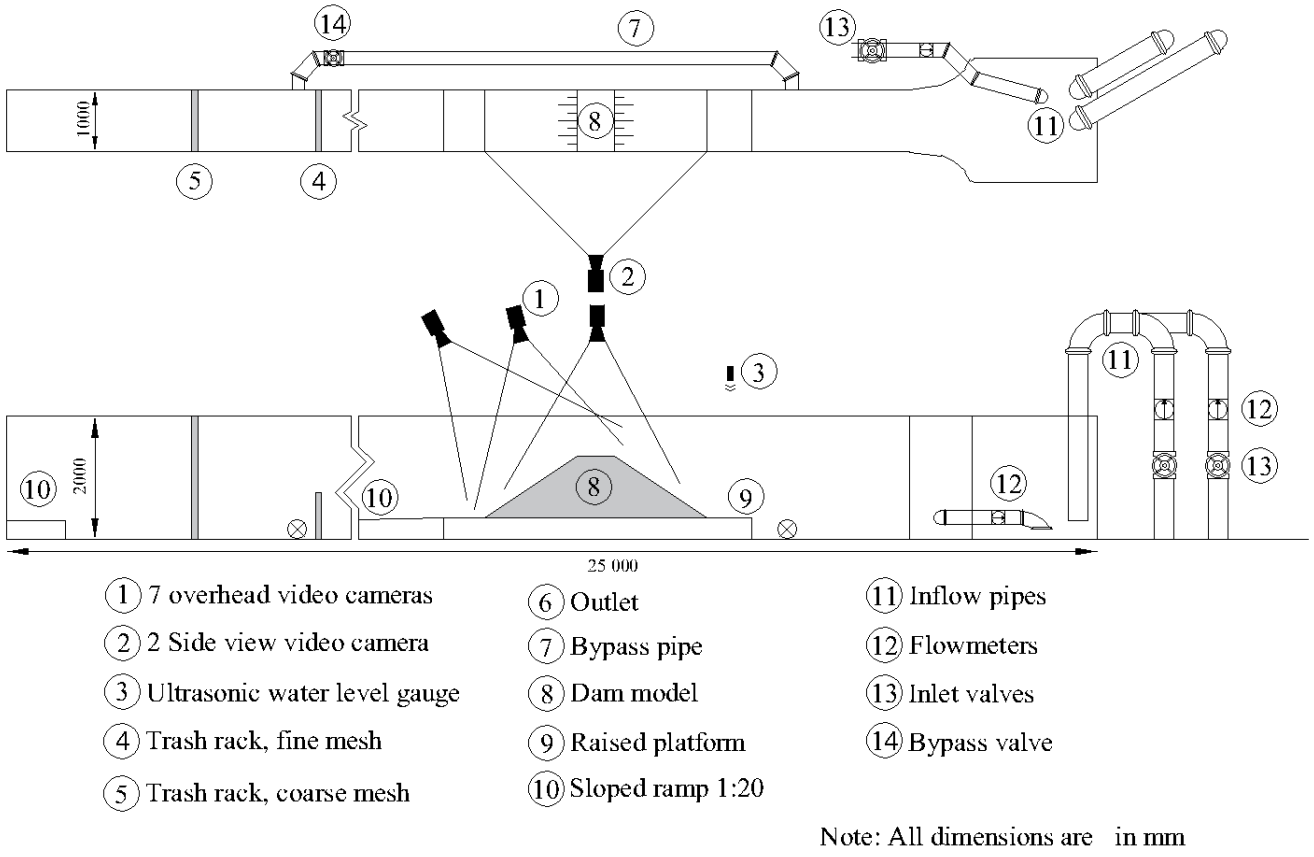

Figure 3.1: Plan and sectional view of model setup (Senarathna 2021)

Figure 3.2: Model setup at NTNU Lab

Ten metal pipes were installed on the top of the aluminium platform to measure the pressure development across the dam section refer to figure 3.3. One metal pipe is 0.25 m away(towards upstream) from the upstream toe to measure the water level in the reservoir. There were two metal pipes just upstream and downstream side of the core to measure the pressure developed in the core on the upstream and downstream side, while other seven pipes were installed on the downstream side of the core approximately at a space of 0.20 m to measure the pressure developed at a different time and discharge during the experiment. These metal pipes were connected to the rubber pipes along the bottom edges of the platform; rubber pipes were further connected to pressure transducers on the outer side of the flume. The pressure sensors produce a voltage in 100 HZ frequency based on the water column in a dam. These produced voltages were fed into the computer with the help of ab Agilent U2355A model data acquisition device, and then voltages data were converted to readable pressure data with the help of the computer.

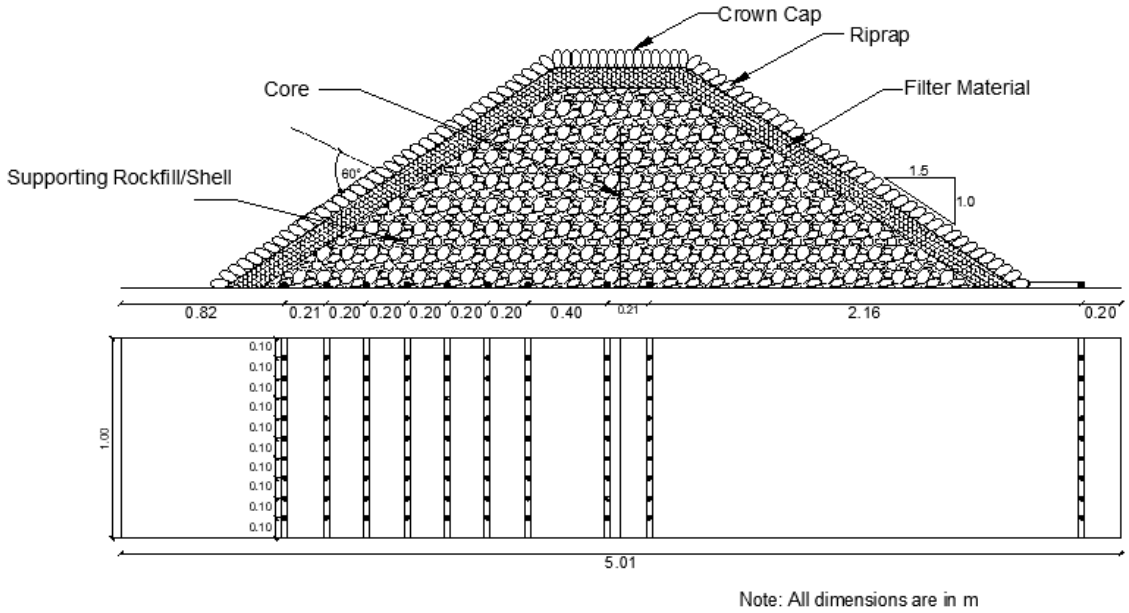

Figure 3.3: Plan and sectional view of pressure sensor

3.2 Material

The material was not prepared during this thesis and used the same material prepared by (Senarathna 2021) during his master thesis. Grain size distribution for rock fill material was established based on existing rockfill dams in Norway by the (NVE 2012). The grain size curve was downscaled at a ratio of 1:10 for this test. However, there was a limitation for the finest material not smaller than 0.5mm. In the installed pump system, if the particle size was greater than 0.5 mm, it would settle in the reservoir. Due to this reason, the material gradation for this test lies on the coarse side of the range, which is shown in figure 3.4.

The material was collected from a local quarry site and a combination of mechanically crushed gabbro, granite, and greenschist. This bulk material was sieved, weighed, and mixed to get proper gradation for shoulder and filter material. Fine material and dust were removed by wet sieve while the coarser material was cleaned by using a concrete mixer. The reason for removing the dust was to keep the water in the pump reservoir clean during the experiment and to prevent the fine material from depositing in the pump reservoir. The Final supporting material was around 4500 kg.

The size of the filter and riprap material was determined based on NVE guidelines and a scale of 1:10, just like other shoulder materials. Some stone sizes in shoulder

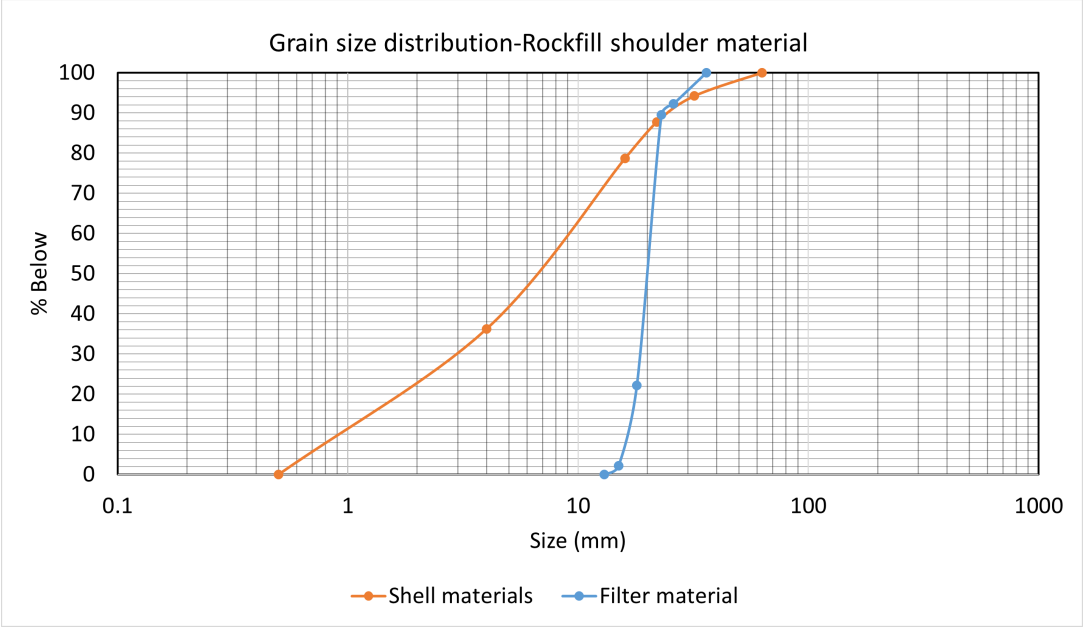

Figure 3.4: Gradation curves for shell material.

material were the size of riprap; it was hard to differentiate between riprap and bigger shoulder material. To solve this problem, the riprap material was painted red so it could be easily identified during the cleaning process.

The riprap and filter material densities were approximately 2600 kg/m^3 and 3050 kg/m^3, respectively. A summary of material properties for the riprap and filter material is shown in the table (3.1). The longest, intermediate, and shortest axes were denoted by a, b and c, respectively. This size was measured for individual stones. The corresponding mean diameter was calculated using equation 2.2; also the stone weight was measured by using a weight scale.

Table 3.1: Summary of riprap material properties (Senarathna 2021)

	Mean Size $[mm]$	**Eq. Dia.** $[m]$	**Weight** $[g]$	**Volume** $[mm^3]$	**Density** $[kg/m^3]$
No. of measurements	550	550	410	50	50
Average	61.7	57.9	250.4	98304	2595
Maximum	78.9	73.57	397.10	123600	2854.00
Medium	61.40	57.44	242.70	97000	2550
Minimum	50.60	46.33	163.19	73600	2494.26

3.3 Construction

The dam dimension was outlined in a flume on the right bank with the help of yellow paint and on the glass side with the help of a permanent green marker. To give an outline for compaction of shell material, it was painted on 0.1 m layers up to 1 m in height in addition there were 12 cm lines drawn on the wall at an angle of 60^o slope to provide an outline for riprap. This is shown in the figure 3.5

In figure 3.5 author of this thesis was cleaning the pressure sensor pipe with the help of a high water pressure jet; the problem with these pressure sensor pipes was they clogged after each experiment test. The shell material was brought downstream of the dam with the help of a crane, and from the downstream side, the material was transported to the dam with the help of a wheelbarrow. Shell material was placed in every 0.10 m layer, and after that, they were compacted by a tamping rod to minimize the void in the shell material. In the figure below, we can see the wooden beam at the center of the pipe; this was used for supporting the rubber core membrane. In the wall, the side membrane was attached with strong tape, and on the glass side, it was attached with weak transparent tape. The reason for using weak transparent tape on the glass side was we wanted to capture the breach of a dam on the glass side, not on the wall side.

Figure 3.5: Cleaning of pressure sensure pipe left and Shell material with rubber core membrane on right, camera facing d/s and u/s side respectively

If we place the filter material bag in the beginning, it will hinder the movement of shell material during construction. After completion of shell material construction, the filter material was placed inside the flume with the help of a crane. This filter material was filled up in the small bucket, and from the bucket to the top of the shell material, the thickness of the shell material was 0.10 m.

In a similar way to filter material, the riprap material was transported to the flume. These riprap materials were filled up in the bucket, and the placing of riprap was on the top of the filter material depending on its type. For dumped riprap, we can dump it from the bucket to the filter material, while for the placed riprap, we need to place it by hand in a very careful manner; stones at the toe were placed horizontally while the remaining stones on the side slopes were placed with the longest axis at an angle of 60^o, the placement of placed riprap was similar with the test carried out by (Ravindra, Sigtryggsdóttir et al. 2019).

In figure 3.6, we can see that the filter material was placed on the top of the shell material and the top of the filter material placement of riprap. This is placed riprap in the given figure, the author of this thesis, was standing in front of the dam to visualize its scale.

Figure 3.6: Completion of Dam Construction

3.3.1 Tests for Analysis

The author was involved in constructing and testing eight dam models; however,, only dams with riprap were taken for analysis and shown in table 3.2 below.

Table 3.2: Conducted test for Analysis

Test	Riprap Type	Camera
M1	Dumped(double layer)	6
M2	Dumped(single layer)	9
M3	Placed(single layer)	9

3.4 Testing procedure

If the test needs to be done after a few days of construction, we need to ensure that the dam body is saturated well. In dry conditions, cohesive forces between particles in the dam may be diminished, leading to early collapse at low discharge. In our case, the test usually took place after a few days of construction, so the dam was watered to make it moist. Then the pressure sensor pipes need to be calibrated. There was a bucket at the top of the flume through which water was passed to the sensor pipe to remove all the entrained air bubbles inside the pipe and calibrate the pressure value to zero.

In tests M1, there were six cameras (Sony Cybershot RX0 / RX0 II shown in figure 3.7 installed to monitor the breaching process, one camera from the glass wall side, and the remaining five from the wooden frame placed on the top of the flume. In tests M2 and M3, there were nine cameras installed; one extra camera was set on the toe side from the glass side and two extra cameras on the wooden frame. At the start and end of the test number of images were taken from the DSLR camera to identify the changes in the dam before and after the test. The bypass valve on the downstream side was closed, then the opening of inflow pump, and the water in the reservoir was filled up to the core level(0.8 m from the bottom of the dam) to see whether the leakage was significant in the structure. Then the cameras were switched on to record the test; these cameras were synchronized with the help of a stopwatch. Usually, the pump filling rate started from 10-15 l/s and increased the discharge by 5 l/s every 30-minute interval.

Installed pressure sensors were Siemens SITRANS P210 pressure gauges; this sensor contains a measuring cell that regularly creates an output voltage linear to the pressure measurement. These voltages and pressure were measured and recorded by Agilent Measurement Manager model U2355A. The data collection was done at 100HZ frequency from each pressure sensor. The flow rate in a pump was measured by Siemens SITRANS FM MAG 5000 microprocessor-based transmitters and the water level were continuously measured by an acoustic sensor on

Figure 3.7: Sony Camera RX0/ROXOII on the left and wooden frame for camera stand on right

the upstream side of the dam. These data were fed into the computer.

When the dam failure process was completed, the inflow pump was closed; then bypass valve was opened to drain the water in the upstream reservoir. Then the photos of the breached dam were again taken by DSLR camera. Some geometric measurements were also done manually at a distance of 0.5 m space along the length flume and at a distance of 0.25 m along the width of the dam. At this time, all the material riprap, filter, and shoulder were completely mixed and sprayed along the flume. First, these riprap materials were collected and separated by hand. In our case, we have to separate filter material around 50 small buckets(capacity of 10 l) from shoulder material. This separation process was done in the sieving bed as shown in the figure 3.8 below.

Figure 3.8: Riprap, shell, and filter material mixed after dam breach

Chapter 4

Analysis and Results

This section discusses failure mechanism due to overtopping, breach development process, breach development rate for both placed and dumped riprap, pore water pressure development in the different models just before and after the breach, and their comparison. PIV analysis for the velocity calculation of particles during the breach, comparison of breaching nature in placed and dumped riprap. Breach parameters calculation for dumped riprap from different empirical equations and their reliability check. Relation between inflow breach discharge and outflow breach discharge, the significance of peak outflow flood during breach action.

Three tests were taken for analysis in this thesis, two of them are dumped riprap and one is placed riprap.A summary of the tests is shown in Table 4.1

Table 4.1: Summary of model tests

Test	Riprap Type	Breach Discharge [l/s]	Camera [Nos.]	Ramping Interval [min]
M1	Dumped(double layer)	30	6	30
M2	Dumped(single layer)	20	9	30
M3	Placed(single layer)	25	9	30

4.1 Placed Riprap

4.1.1 Failure Mechanism due to overtopping

The experiment M3 was captured from 9 cameras, and through the very fine time step(8 images per second), it was observed that the failure started on the downstream edge of the crest where aeration was absent, which is very much in agreement with (Hiller 2017). Ongoing through the video footage taken during the experiment, the overtopping discharge created extra force on the downstream toe of the dam. At a certain point, the toe was not able to take more force from the overtopping discharge, and the developing gap was observed on the downstream edge of the crest. This developing gap was observed due to compaction of riprap material, and exposure of the filter material resulted in the sliding of the riprap on the downstream side shown in figure 4.2 , which is similar to the failure mechanism described by (Siebel 2007).

This test M3 was identical to the test conducted by (Senarathna 2021) in his master thesis; however, the breaching discharge for him was 55 l/s which is a very high breaching discharge compared to this experiment. We tried to figure out what could be the reason for such a large difference, and we found that in this test, the geotextile was only up to the shell membrane and not extended up to the filter and riprap material which causes lower friction between riprap, filter to the ground surface leading to breach at lower discharge.

Figure 4.1: Placed riprap exposed to overtopping before sliding, t=20 s

Figure 4.2: Sliding in placed riprap due to overtopping,t=25 s

4.1.2 Breach Development Process

The video footage taken from the glass side was used to understand the breach development and progress in the dam. This video was clipped to the shorter period, which shows sometime before the breaching start point to the breach ceasing point. The VLC media player was used to extract the images every five seconds so that we could observe the time-lapse of breach development refer to figure 4.3. Qgis was used to relate the pixel coordinates and real coordinates; in Qgis, there is the geo-reference command on which we need to import the dam images. We have to assign at least four coordinate points in the image to get a proper referencing system then Qgis will give us corresponding pixel coordinates. These pixel and real coordinates are imported in the R programming language; we have to run a code that will convert the extracted images to TIF images. These TIF images will have real coordinate systems and be imported to the QGIS to draw the failure progress in the dam, which is shown in figure 4.4.

The dam M3 was first filled up to the core level to see whether the dam had considerable leakage or not. After confirmation, the dam did not have more leakage; the dam was overtopped with the discharge of 15 l/s and waited for 30 minutes to see whether this discharge initiated breaching. Then the discharge was increased by 5 l/s every 30 minutes interval. The dam didn't break for more than 1 hour; it revealed that the dam would not breach until the overflow discharge had enough energy, which is in agreement with (Zhenming et al. 2022). When the discharge reached to 25 l/s, the riprap started to erode, leading to exposure of filter material; when filter material gets exposed, the breaching rate increase rapidly. We can see in figure 4.3 that the breach started at 20 s time, and in the next 20 s time

interval, all the material up to the crest was eroded. In the crest, the erosion rate was higher due to the steeper slope in the crest part compared to the toe part. After erosion up to crest level, the eroded downstream slope was milder, and the erosion rate decreased slowly. From time 60 s, the erosion rate decreased it is due to the rise of the level on the downstream side, causing a gentle slope for erosion. From the time interval, 300 s, it took the next 450 s to see a significant difference in the erosion process; after 750 s, the erosion started to cease, and after 975 s time interval, the stable flow was maintained.

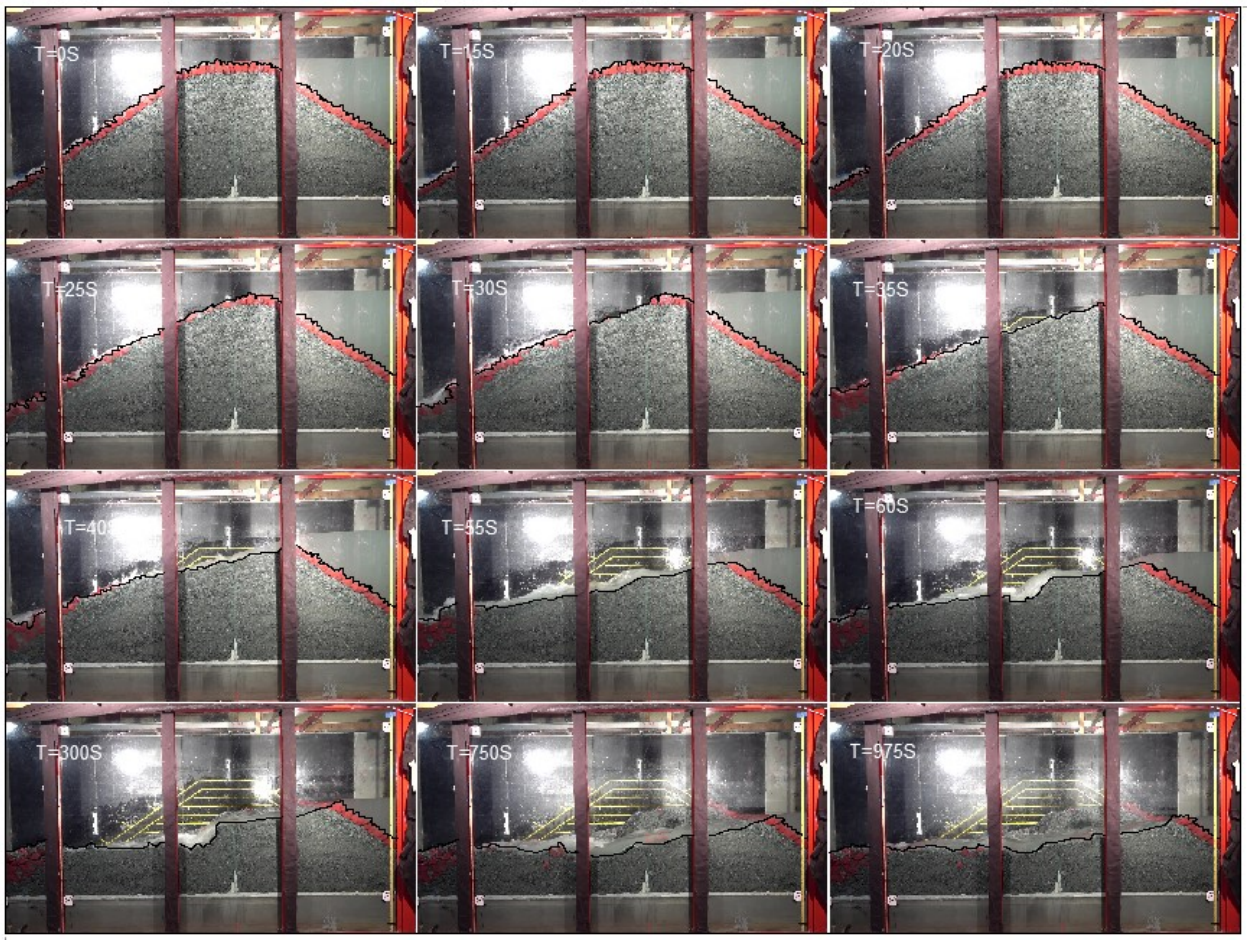

Figure 4.3: Breaching process in placed riprap

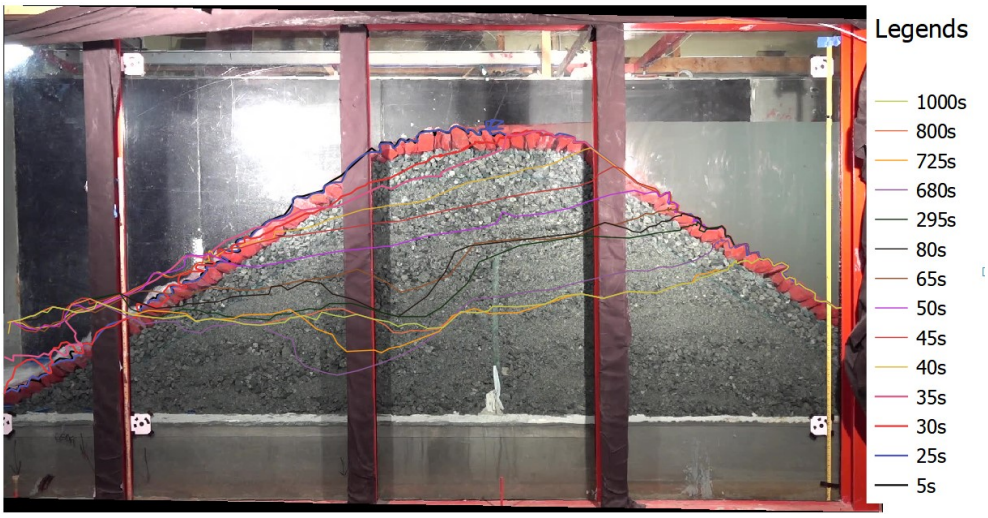

Figure 4.4: Temporal evolution of breach process in placed riprap

Toe support in a rockfill dam is crucial from the stability point of view. Usually, the breach starts on overtopping if toe support is not able to take more force from overtopping discharge (Ravindra, Sigtryggsdóttir et al. 2019). To understand the breaching process in toe support, one separate camera was used. The breach development process at the toe is shown in figure 4.5. In periods 0,20,40 s, we can see there was no movement of the riprap on the toe support; at a time of 45 s, the sliding at toe occurred, leading to the breaching of the dam. When the breaching process continues, more riprap on the toe starts to accumulate and provides more stability. After the 150 s, there was no significant further erosion on the downstream toe side; however, the erosion on the upstream side continued for a longer time period.

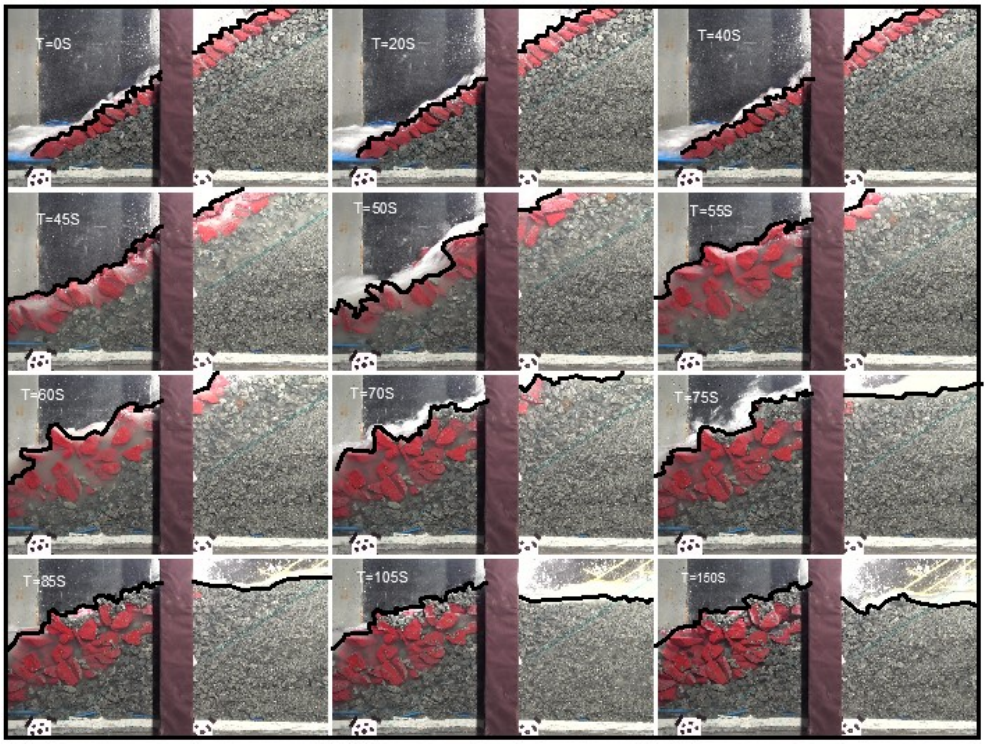

Figure 4.5: Breaching process at toe in placed riprap

4.1.3 Breach Development Rate

TIF images developed from R programming languages were imported to Q gis, and the failure surface was drawn into these images. To define the breach development rate, the reference point was taken as crest centre and 1 m d/s from crest centre at a time period 0 s.

It was observed that the major erosion rate started from the 30 s to 50 s time interval refer to table 4.2. This indicates that the breaching of the rockfill dam is very quick, which may cause inundation and big floods on the downstream side. At a time of 30 s, the erosion rate at the crest was around 11 mm/s; however, at 1 m d/s from the crest, there was no significant erosion rate. At time 35 s, the deposition occurred in the 1 m d/s; it was due to the transfer of material from the crest to the toe. From the figure below, we can see that the maximum erosion rate at the crest was between the period the 40 s to 50 s and found to be 20 mm/s; however, at 1 m d/s maximum breach rate was 18 mm/s at a time 50 s. The breach starts to cease from time 80 s for both reference points; this can be observed in figure 4.6.

Table 4.2: Vertical Breach rate in placed riprap

Time	Height(mm)		Breach rate (mm/s)	
	at crest	1 m d/s from crest	at crest	1 m d/s from crest
0	1200	750	0	0
25	1200	750	0.00	0.00
30	1146	747	10.80	0.60
35	1090	782	11.20	-7.00
40	990	733	20.00	9.80
45	895	720	19.00	2.60
50	798	632	19.40	17.60
65	734	532	4.27	6.67
80	731	513	0.20	1.27
295	664	423	0.31	0.42
680	444	390	0.57	0.09
725	433	430	0.24	-0.89
800	461	396	-0.37	0.45
1000	459	391	0.01	0.03

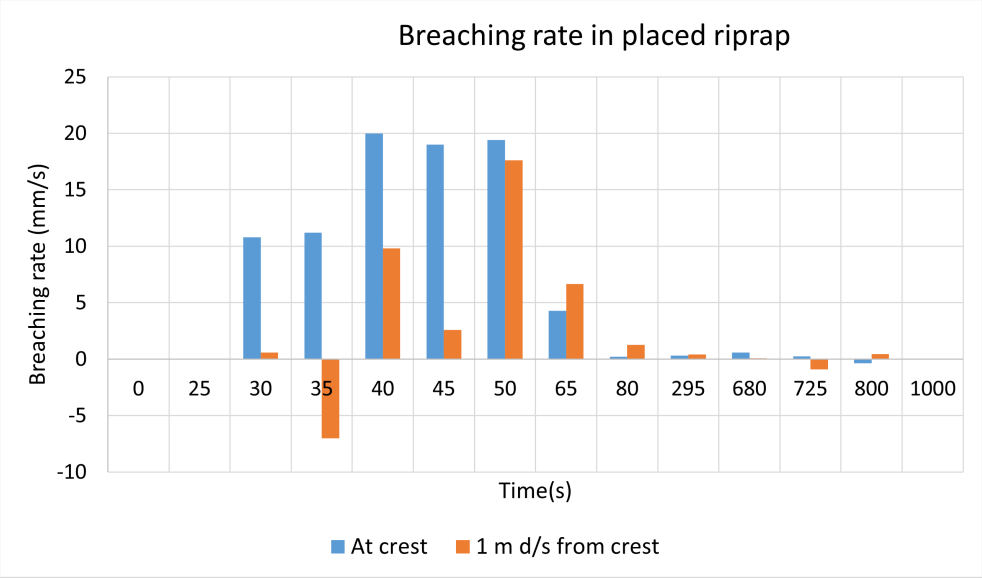

Figure 4.6: Vertical Breaching rate in placed riprap

4.2 Dumped Riprap

4.2.1 Failure mechanism due to Overtopping

Six cameras captured the dam model M1 (dumped double layer) while nine captured model M2 (dumped single layer). In model M2, there was one extra camera on the toe of the dam and two more cameras for the top view. Similar to placed riprap, both single and double layers breached just downstream side of the crest; however, there is no such aeration like in placed riprap just before breach shown in figure 4.7 and 4.8. Ongoing through the video footage for both single and double layer riprap dams in small time intervals, it was found that initial breach starts, and minor sliding occurs. This sliding stabilizes for the ceratin period; in our case, the major continuous sliding starts after 5-10 seconds . In placed riprap, the riprap behaves as a single unit, and when sliding occurs, all the riprap material gets deposited in the toe of the dam shown in figure 4.5 while for the case of dumped riprap, it was found that there was no such deposition of riprap at the end.

The breaching discharge for single layer and double dumped riprap was 20 l/s and 30 l/s, respectively. It indicates that the double layer dumped riprap has a much higher breaching discharge capacity than the single-layer dumped riprap. The placement of placed riprap is time-consuming and requires technical skills. If riprap can be easily found from the quarry site, then double layer riprap may be the solution for a similar kind of breaching discharge as placed riprap.

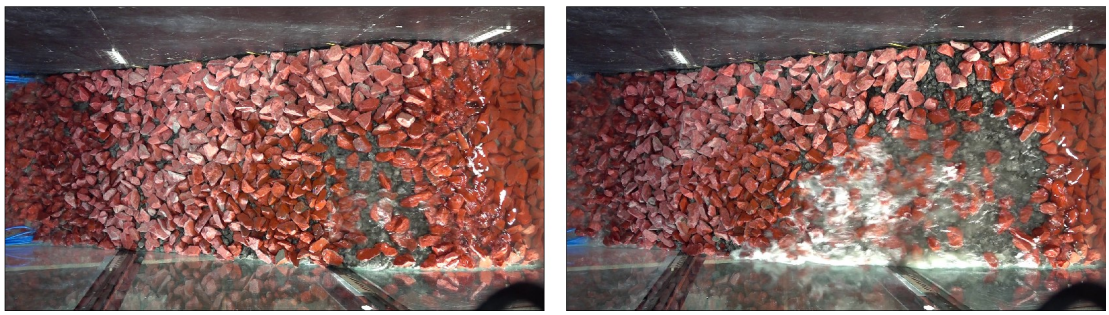

Figure 4.7: Single layer dumped riprap exposed to overtopping during sliding(left,t=5 S) and afer sliding(right, t= 10s)

Figure 4.8: Double layer dumped riprap exposed to overtopping before sliding(left,t= 0 s) and during sliding(right,t= 10 s)

4.2.2 Breach Development Process

The process for generating TIF images and importing them to QGIS to draw the failure surface is the same as described for placed riprap. Usually, a single layer dumped riprap is weaker than a placed layer or dumped double-layer riprap with lower breaching discharge. The dam started to overtop with a low discharge of 10 l/s compared to placed riprap and increased by 5 l/s every 30 minutes time interval. The breach was initiated at 20 l/s discharge at a time of 10 s and then temporary stability until the 20 s. After the continuous breaching start, the breaching rate wass much higher from the 20 s to 50 s time interval. From the 65s time interval, the breach rate decreased, and from the 165 s breaching, the rate decreased further. Then from time interval 715 s, the breaching process ceased and maintained the normal through the dam shown in figure 4.9. The total breaching time period for a single layer was 715 s, and for placed riprap, it was 975 s, which is due to the difference in breaching discharge. High breaching discharge leads to erosion for a longer time period.

All the failure line surfaces from figure 4.9 is compiled into figure 4.10 to see the temporal evolution of the breaching process describes the temporal evolution of breaching process.

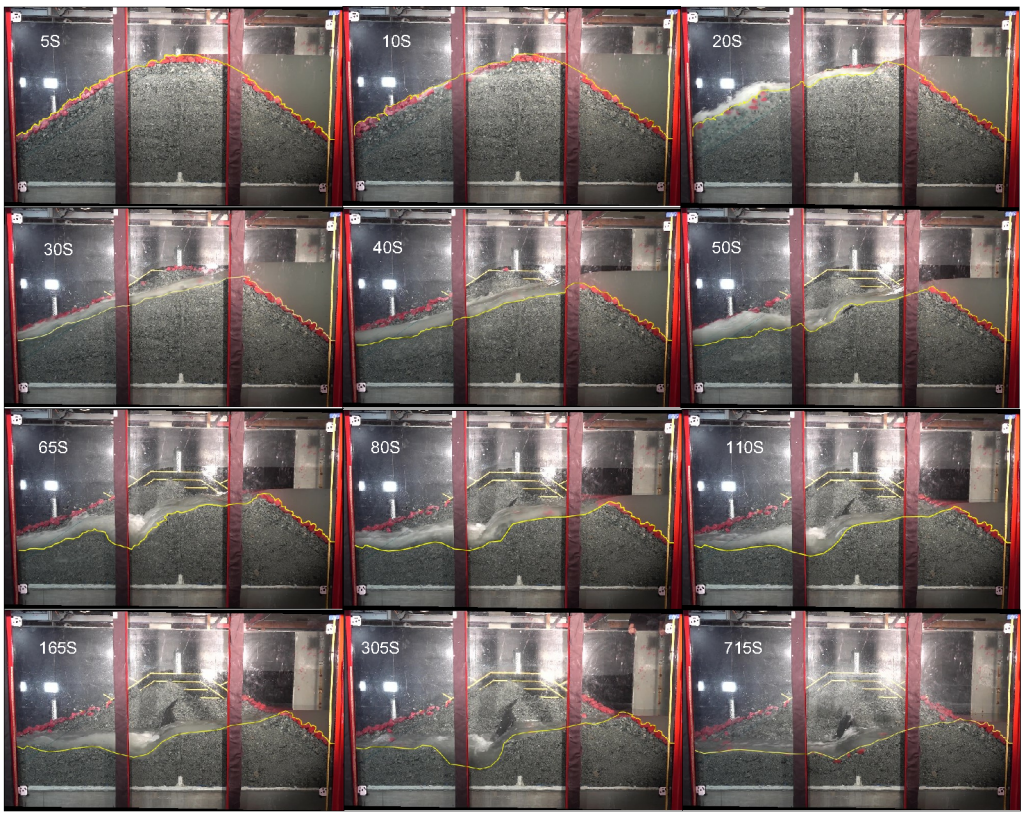

Figure 4.9: Breaching process in single layer dumped riprap

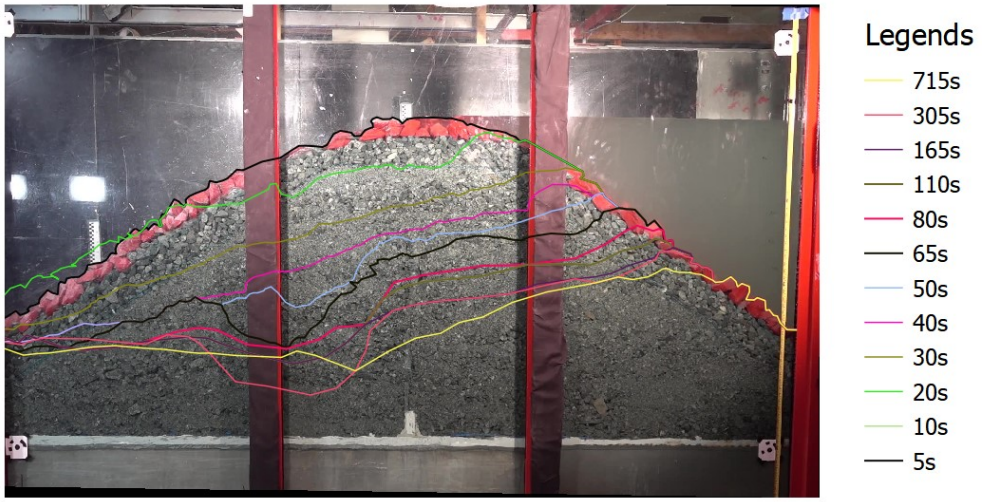

Figure 4.10: Temporal evolution of breaching process in single layer dumped riprap

In double layer dumped riprap, the model started to overtop with breaching discharge of 15 l/s and increased by 5 l/s in every 30-minute time interval, same as another riprap above. The failure mechanism in double-layer dumped riprap was similar to single-layer dumped riprap. The dam surface profile can be comparable; at period 65 s, there was the formation of a u section in the dam for both single layer and double layer dumped riprap. The breaching process time, in this case, was a little higher compared to single-layer riprap and similar to placed riprap. The breaching process is shown in figure 4.11 and the temporal evolution of the breaching process is shown in figure 4.12

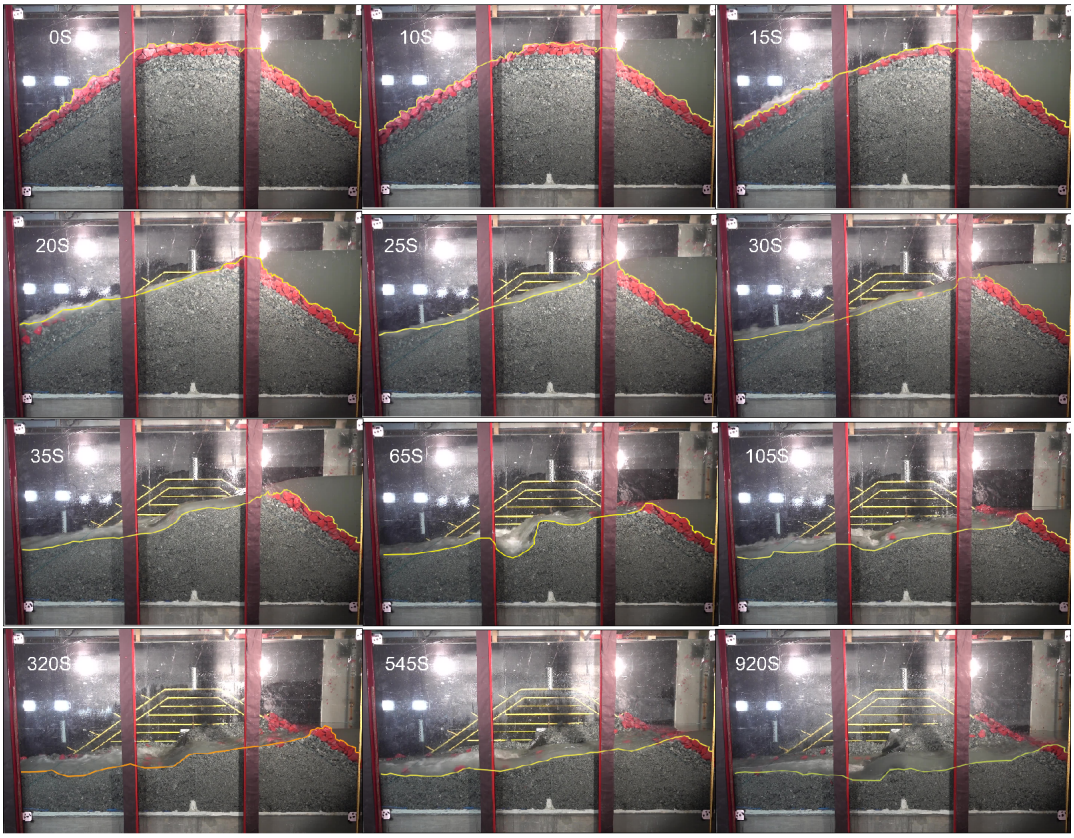

Figure 4.11: Breaching process in double-layer dumped riprap

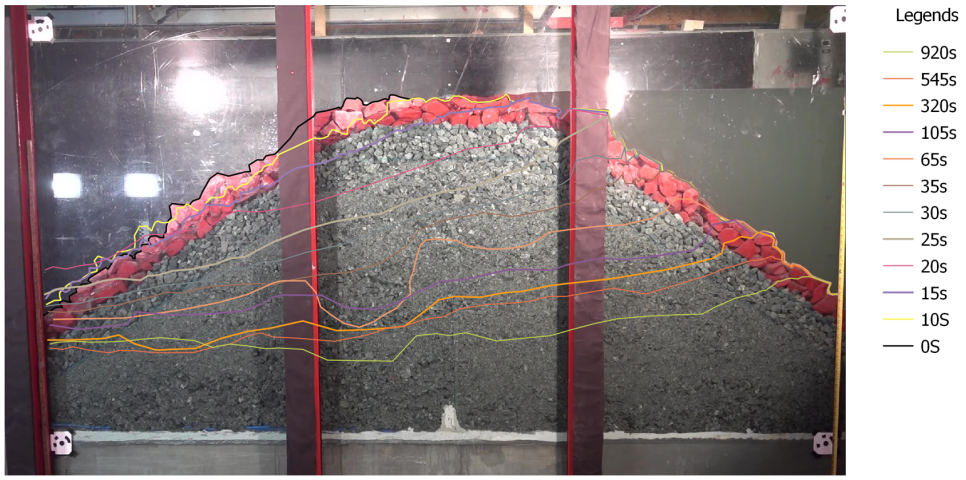

Figure 4.12: Temporal evolution of breaching process in double layer dumped riprap

4.2.3 Breach Development Rate

Similar to mention in placed riprap, the TIF images generated from R programming were imported to Qgis, and failure surfaces were drawn. Taking reference to 0 s and at a crest position, the erosion rate was determined. Referring to the figure 4.13 and table 4.3, we can see that the erosion rate in single layer riprap was higher in the 20 s time interval; it was due to failure in single riprap started earlier. In time the 30 s the breaching rate in double-layer riprap was much higher; it is almost double the highest breaching rate in single-layer riprap. From time 165s, the erosion rate decreased significantly, and after 715 s, the erosion rate ceased almost in both dams, which are shown in figure 4.13.

Table 4.3: Vertical Breach rate in dumped riprap

Time	Model M2 at crest	Breach rate [mm/s]	Time [s]	Model M1 at crest	Breach rate [mm/s]
0	1181	0	0	1248	0
10	1181	0.00	10	1248	0.00
20	1008	17.30	15	1194	10.80
30	863	14.50	20	1043	30.20
40	773	9.00	25	915	25.60
50	734	3.90	30	837	15.60
65	681	3.53	35	809	5.60
80	602	5.27	65	718	3.03
110	580	0.73	105	576	3.55
165	501	1.44	320	511	0.30
305	498	0.02	545	473	0.17
715	366	0.32	820	376	0.35

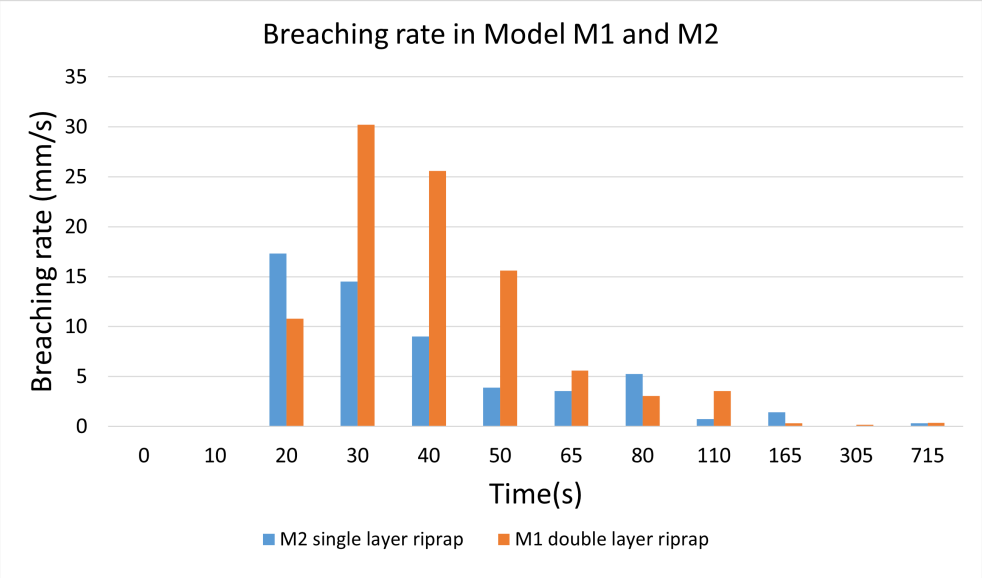

Figure 4.13: Vertical Breaching rate in dumped riprap

4.3 Comparison of breaching discharge and Failure mechanism with Ravindra and Sigtryggsdottir (2021)

In a similar type of experiment conducted by Ravindra and Sigtryggsdottir (2021)), it was observed that they have much higher breaching discharges. It was due to the geotextile not extending up to the riprap, causing low friction between the riprap and the ground surface. As from the previous discussion, it is revealed that the toe plays a crucial role in stability point of view; the riprap starts to slide when the toe is not able to take extra force from overtopping discharge. Due to low friction, the toe was not able to take more force and causing to lower breaching discharge. In this study, all the failure mechanism was due to sliding; however, in the case of Ravindra and Sigtryggsdottir (2021), the dumped riprap failed by surface erosion.

Table 4.4: Breaching discharge and Failure mechanism comparison with Ravindra and Sigtryggsdottir (2021)

Riprap Type	Raj(2022)		Ravindra and Sigtryggsdottir (2021)	
	Failure Discharge(l/s)	Failure mechanism	Failure Discharge(l/s)	Failure mechanism
Placed	25	Sliding	60	Sliding
Dumped single layer	20	Sliding	40	Surface erosion
Dumped double layer	30	Sliding	-	-

4.4 Pore water pressure measurements

As mentioned in the previous section, the metal pipe was placed on the bottom of the dam connected wth the rubber pipes. These rubber pipes were further connected to a pressure sensor. These pressure sensors produce 100 voltage values per second based on the water column, and the voltages data were converted to pressure readings in meters. An average of 100 voltage data per second is used for the calculation. Using average data per second, the phreatic surface can be produced throughout the model run. The detailed pressure measurements and inflow discharge is shown in Appendix A.

Table 4.5 describes the pressure developed at the bottom of the dam in different pressure sensors just before the breach for different models. The horizontal distance for the pressure sensor was measured from the downstream toe of shell materials.

Table 4.5: Pore Pressure at bottom of dam before breach

Pressure Pipe	Distance [m]	M1	M2	M3
P10	0.12	0.24	0.20	0.23
p9	0.32	0.35	0.31	0.34
P8	0.52	0.46	0.41	0.44
P7	0.72	0.52	0.47	0.53
P6	0.92	0.60	0.56	0.60
P5	1.12	0.60	0.62	0.65
P4	1.33	0.62	0.65	0.70
P3	1.74	0.65	0.67	0.74
P2	1.94	1.18	1.12	1.18
P1	4.11	1.20	1.18	1.23

Figure 4.14 describes graphically the pore pressure developed at the bottom of the dam just before the breach. There are outlines for the shell material, riprap materials, and filter material for better visualization of the dam body.

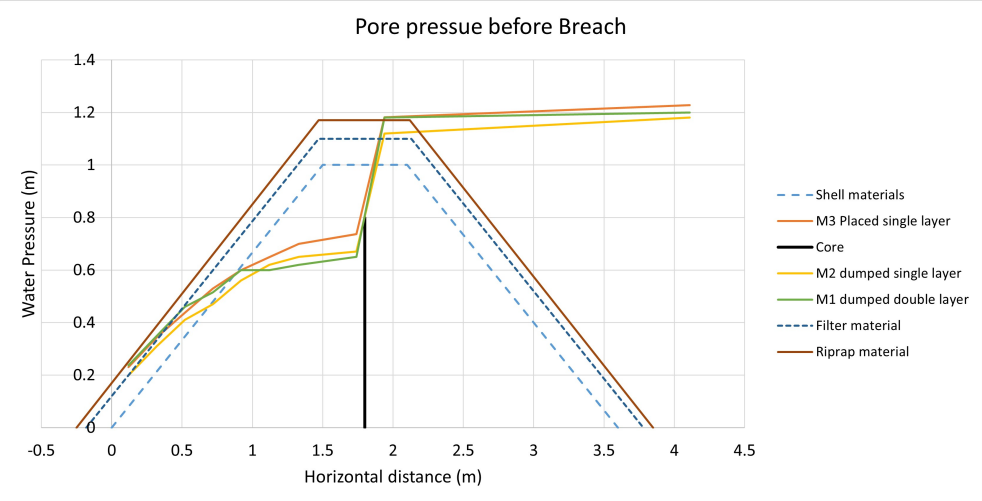

Figure 4.14: Pore pressure at bottom of dam before breach

The pore pressure developed at the breach; in the upstream side of the core membrane, the pressure was the same as before the breach; however, in the downstream part of the core, the pressure increased instantly, it was due to overtopping and erosion of shell material leading to increase the water level. The pressure data is shown in table 4.6 below.

Table 4.6: Pore pressure in dam after Breach

Pressure Pipe	Distance [m]	M1	M2	M3
P10	0.12	0.478	0.382	0.422
P9	0.32	0.53	0.46	0.504
P8	0.52	0.59	0.52	0.558
P7	0.72	0.612	0.57	0.61
P6	0.92	0.68	0.66	0.668
P5	1.12	0.67	0.71	0.708
P4	1.33	0.69	0.71	0.732
P3	1.74	0.71	0.71	0.769
P2	1.94	1.18	1.12	1.182
P1	4.11	1.2	1.18	1.228

Figure 4.15 describes graphically the pore pressure developed at the bottom of the dam just before the breach. In all three cases, we can observe that the breach only starts after overtopping riprap material.

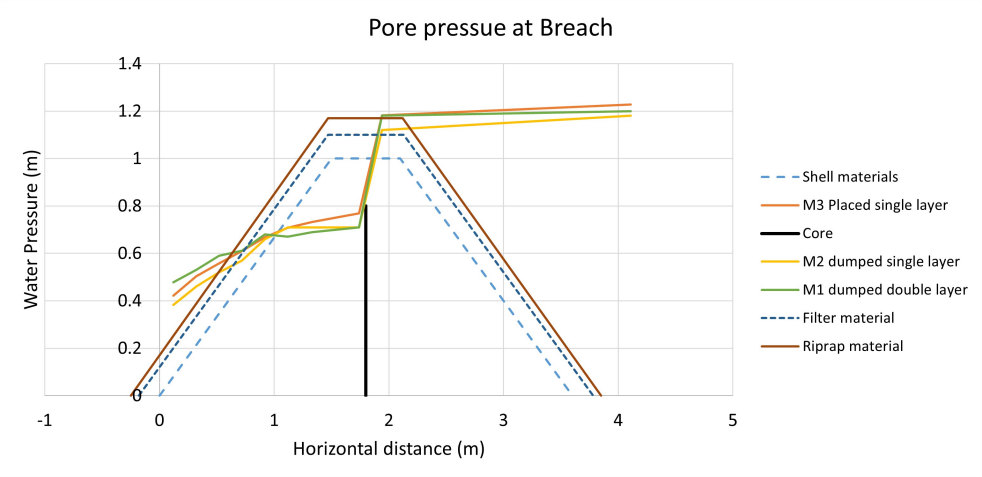

Figure 4.15: Pore pressure at bottom of dam at breach

4.5 PIV Analysis

It is difficult to measure the velocity of particles during dam breaching; however, velocity calculation of particles during particle movement is important for describing the failure mechanism and finding the location where the breach initiates. One

of the easy and accurate ways of measuring the velocity and discharge is by using PIV(particle image velocity) analysis. There are different software available for the calculation of particle velocity. This thesis uses FUDAA PIV analysis for calculation; FUDAA is freely available, powerful, and user-friendly software.

4.5.1 Description to run FUDAA piv analysis

On opening the FUDAA analysis software on the top menu, there is an images option; on clicking the images option, we can see an imported image from the video. Now we need to import the video footage containing the dam breach; after importing the video, there is an option to keep a number of images per second. In this thesis, I have used 1 image in every 1s interval; it depends on the particle's movement. We can also choose the start and ending period of video footage. Then video images will appear in 2D view space, and you can move the images in the different time frames. If the images are affected by the shaking during video record time, then you need to stabilize the images; on clicking images on the menu bar, you can see an image stabilization option. Avoiding movement by using a tripod and attaching the camera to a stable support is always a better idea.

We need to click the orthorectification option in the menu bar to correct the images from perspective distortion and assign a metric size to the pixel. There we have to add some ground reference points; at least four are necessary for 2d calculation, then we have to verify the reference points. On just right side of orthorectification in the menu bar, we can see LSPIV analysis. On clicking it, we can see calculation parameters. Then we have to define the interrogation and search area; it depends upon the size of the flow area in video footage. Then we have to define the grid points; these grid points can be adjusted, and in each grid node, we will get velocity. In post-processing mode, we can apply filters to the velocity result, calculate the time average, and calculate the streamlines.

4.5.2 PIV Results

Four PIV analyses were done, two for placed riprap and two for dumped riprap. It was found that the observation between two dumped riprap was similar while observation with placed riprap was different. The placed riprap occurs more abruptly than the dumped riprap, which is in agreement with (Ravindra, Gronz et al. 2020). In both placed and dumped, riprap failure started on the crest's downstream side, which is similar to the observation made through the number of images as discussed in sections 4.1.1 and 4.2.1 above.

In placed riprap, the failure discharge was 25 l/s, and the velocity of particles was found in the range of 0-0.3 m/s and noted that this first maximum velocity occurred in the first sliding(breach initiation) time, and this maximum velocity was

Table 4.7: Breach velocity for different type of riprap

Type of riprap	Breaching discharge [l/s]	Velocity range [m/s]	Max. velocity at breach [m/s]
Single layer placed riprap	25	0-0.30	0.30
Single layer placed riprap toe	25	0-0.16	0.16
Single layer dumped riprap	20	0-0.21	0.18
Double layer dumped riprap	30	0-0.21	0.20

also observed at a different time interval. The velocity range in the toe section of placed riprap is 0-0.16 m/s which is much smaller compared to the slope of placed riprap. It is due to stacking of placed riprap at a toe.

In the case of single-layer dumped riprap, the failure discharge was 20 l/s, and velocity was found in the range of 0-0.21 m/s, which is smaller compared to the placed riprap. Unlike in placed riprap first breach velocity was not the highest; the velocity was around 0.18 m/s, while the maximum breach velocity was observed to be 0.21 m/s.

In double layer dumped riprap, the failure discharge was 30 l/s, and the velocity of the particle during breach was found in the range of 0-0.21 m/s which is similar to the single-layer dumped riprap. Ongoing through the velocity analysis at a different time step, it was found that in double-layer dumped riprap, the velocities of riprap were in the maximum range; most of the riprap velocity was around 0.19 m/s; however, in the case of single-layer riprap, the most of the velocity was around 0.14 m/s. This discussion is also shown in the figure below; particle velocity at different time intervals is shown in Appendix C.

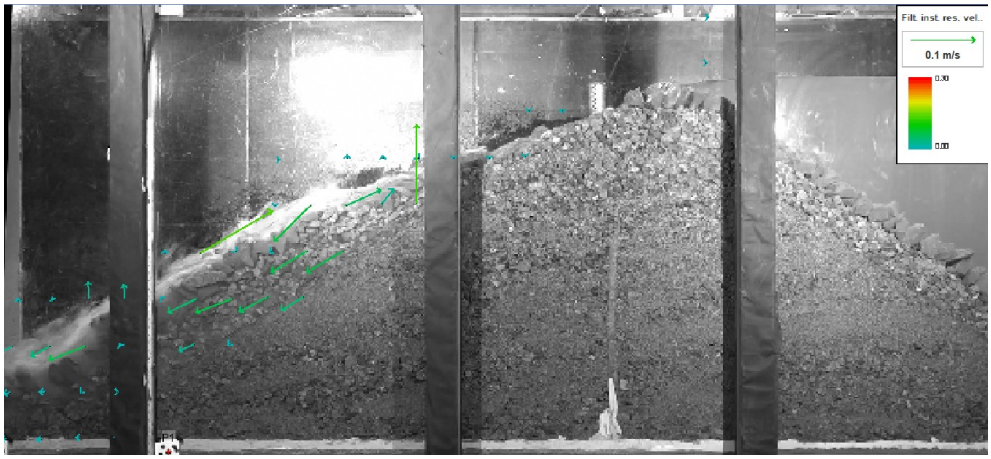

Figure 4.16: PIV analysis of single layer placed riprap

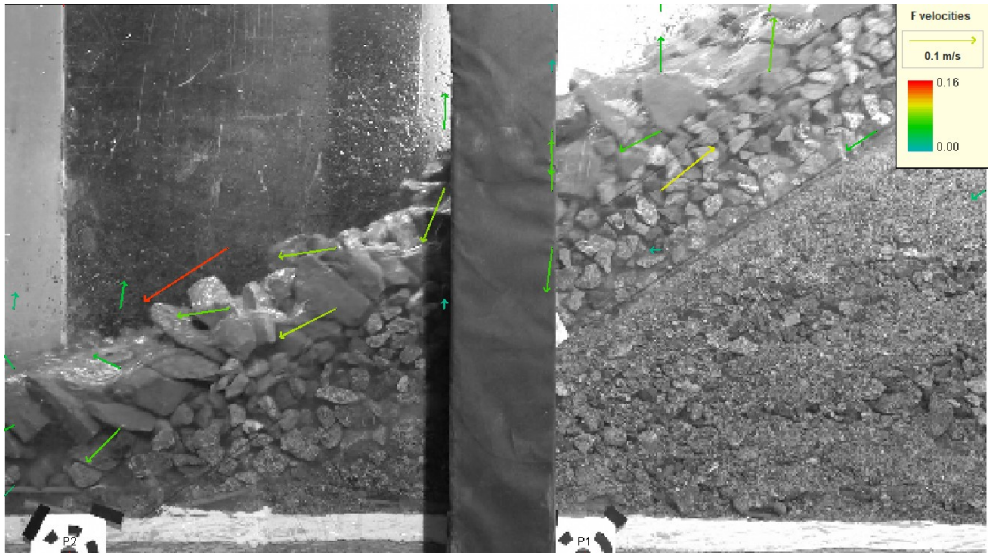

Figure 4.17: PIV analysis of placed riprap toe

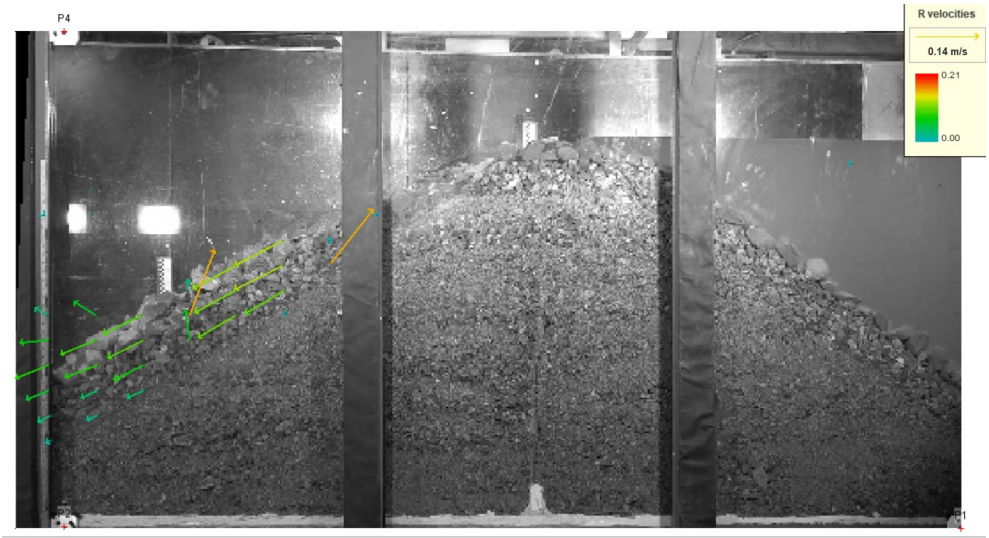

Figure 4.18: PIV analysis of single layer dumped riprap

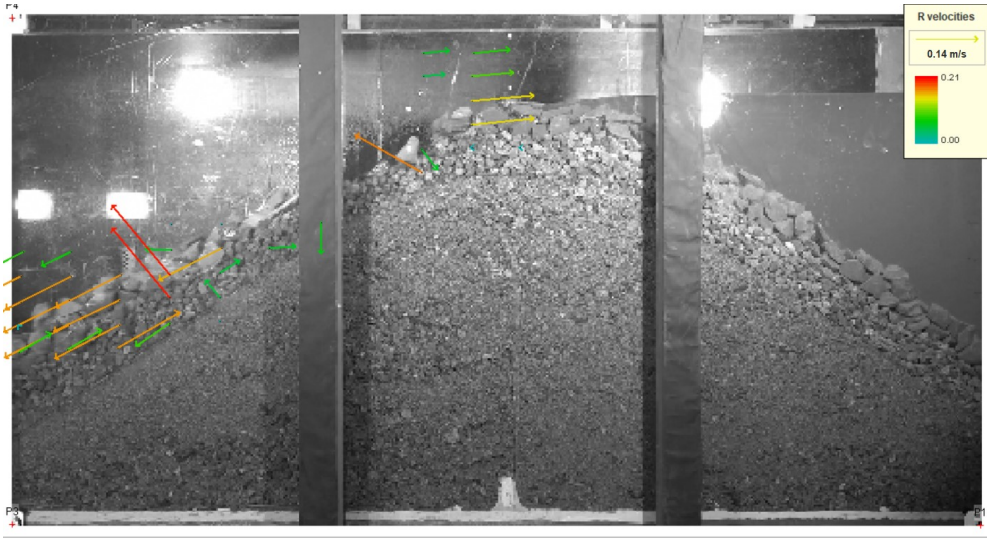

Figure 4.19: PIV analysis of double layers dumped riprap

4.6 Breach Parameters

In this section, we will use the empirical model to find the breach parameters such as breach opening width, peak discharge, and failure time. The above-discussed equation in subsection 2.4.1 is suitable for the earth-fill dams, and there is fewer research conducted on rockfill dams to find the breach parameters, So we will use these equations to find the breach parameter for dumped riprap rockfill dams and will compare the results from equations and data result obtain from the experiment. Then we can check the reliability of the above equation for dumped riprap rockfill dams. Manual breaching width measurement at different chainage is shown in Appendix B.

Data required to calculate breach parameters

Table 4.8 presents the data obtained from the experiment which is required to compute the breach parameters.

Table 4.8: Data reqire to calculate breach parameter

Dam type	h_w [m]	h_b [m_3]	h_d [m]	V_w [m_3]
Dumped single layer riprap	0.848	0.84	1.18	7.136
Dumped double layer riprap	0.912	0.914	1.26	6.886

Average breach width

Table 4.9 provides the breach opening width calculation from different empirical equations; this calculation shows that Xu Zhang (2009) gives the more accurate value for dam breach width; the value obtained from Froehlich(1995a) was almost one-fourth compared to the measured breach width while the US Bureau of reclamation(1998) gave almost one and half times the actual breach opening width.

Table 4.9: Dam breaching width calculation using empirical equations

Reference	Dumped riprap[m]		Equation
	Single layer	Double layer	
Measured	1.44	1.62	
Xu & Zhang (2009)	1.12	1.16	2.12
Froehclich (1995a)	0.44	0.44	2.15
US bureau of reclammation(1988)	2.12	2.28	2.19

Peak Discharge

The peak discharge calculation from different empirical equations is presented in table 4.10 below. The values through these equations are very high compared to observed peak discharge in a lab during experiments.

Table 4.10: Peak Discharge calculation using empirical relation

Reference	Dumped riprap[m3/s]		Equation
	Single layer	Double layer	
Measured	0.074	0.099	
Xu & Zhang (2009)	2.91	3.19	2.13
Froehclich (1995a)	0.88	0.96	2.17
US bureau of reclammation(1988)	14.08	16.11	2.21

Failure time

The failure time calculation from different empirical equations is presented in table 4.10 below. The Xu and Zhang (2009) gave two times more failure time than observed while the failure time calculation from Froehlich (1995a) and U.S.Bureau (1988) was very small. For this experiment, these empirical relations didn't produce satisfactory results.

Table 4.11: Failure time calculation using empirical relatons

Reference	Dumped riprap[hr]		Equation
	Single layer	Double layer	
Measured	0.20	0.25	
Xu & Zhang (2009)	0.60	0.57	2.14
Froehclich (1995a)	0.008	0.008	2.16
US bureau of reclammation(1988)	0.023	0.025	2.20

4.7 Outflow discharge at breach

The breach discharge was measured indirectly; to calculate it, we need to find the stage versus water stored volume in the reservoir. Senarathna (2021) and I had experimented on the same setup at NTNU Lab. He measured the cross-sectional area of the reservoir, incremental increase in volume, and further took into account the water stored in the upstream section of the dam. The porosity of the shell material was measured by filling the material in the known volume of the container and then measuring the water required for the complete saturation of the sample. In the figure 4.20 we can see that there is a marginal difference between a dam without a riprap and filter layer and a dam with these two layers.

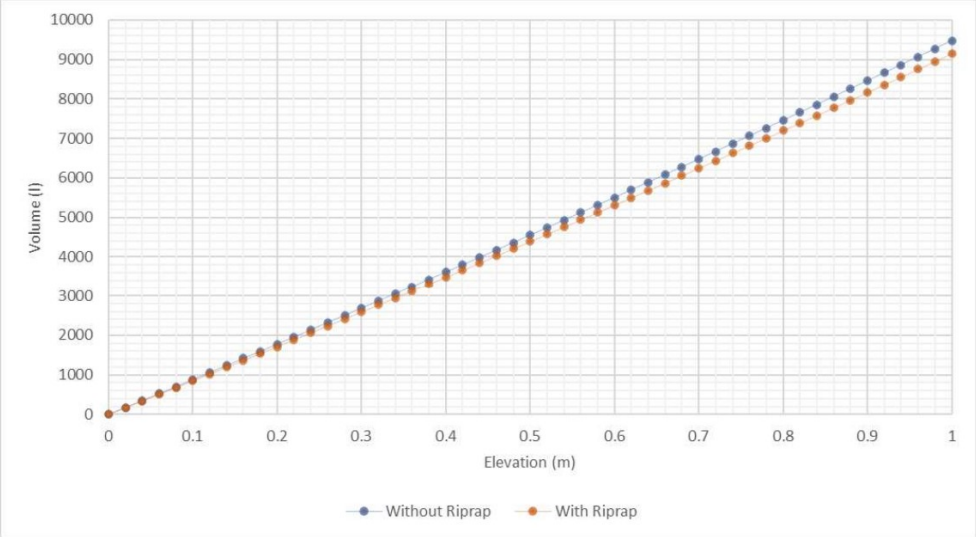

Figure 4.20: Reservoir volume versus elevation without riprap layer and filter layer and with these two layers

During the breach, water elevation on the upstream side of the reservoir was measured by pressure sensors. These pressure sensor data were converted to readable meter reading by R programming language as described in previous sections 3.4 and 4.3. In figure 4.20, we can see that elevation and volume have linear relations. The best-fitting line was plotted, and its equation 4.1 was determined; now, the water level at different periods can be converted to stored water volume in the reservoir. By using a simple water balance equation, we know the difference in water volume in a given time interval; dividing the change in water volume by time interval gives the outflow discharge.

$$V = 9200h \tag{4.1}$$

where: V = Volume of water stored in the reservoir(L)
h = water elevation in (m)

In the figure below, we can see that the peak outflow discharge was observed when the first breach initiation occurred. This was common for all three models. The inflow breach discharge and outflow discharge can be related; the higher the inflow breach discharge higher the outflow breach discharge. Inflow and outflow discharge is shown in the table 4.12 below.

Table 4.12: Inflow vs outflow discharge at breach

Dam type	Breach discharge(l/s)	
	Inflow	Outflow
Placed riprap	25	88
Single layer dumped riprap	20	74
Double layer dumped riprap	30	99

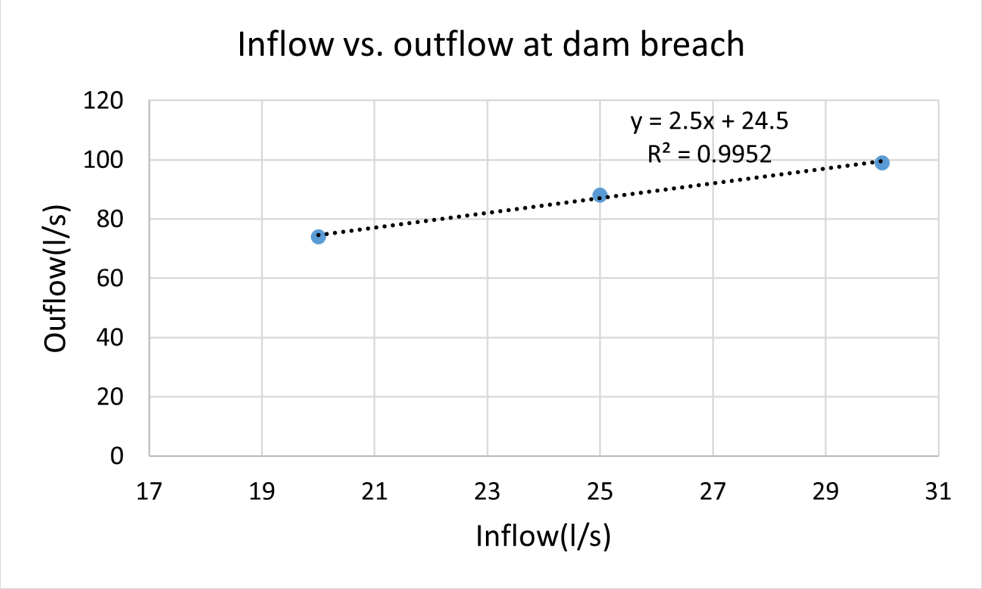

Figure 4.21: Relation between inflow peak discharge and outflow peak discharge

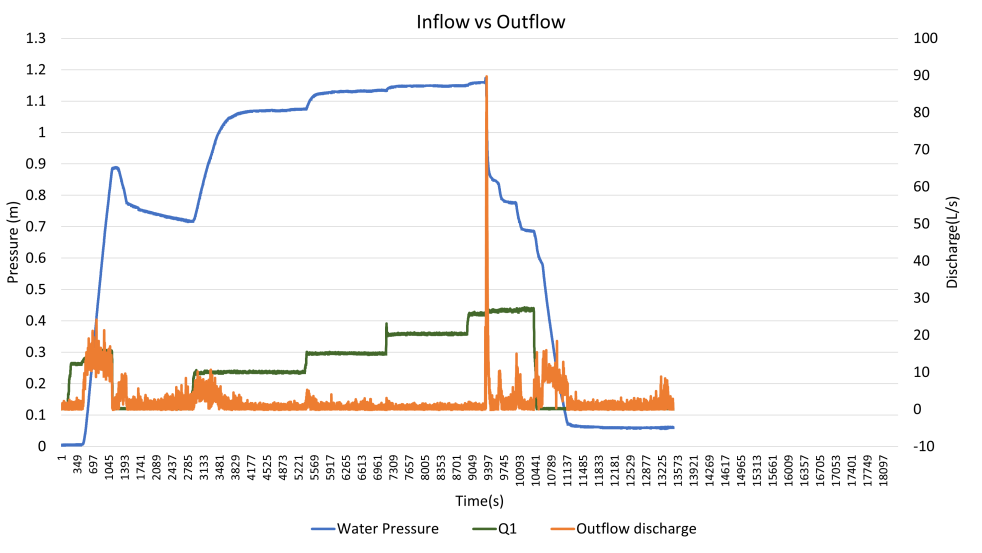

Figure 4.22: Outflow discharge in placed riprap at dam failure

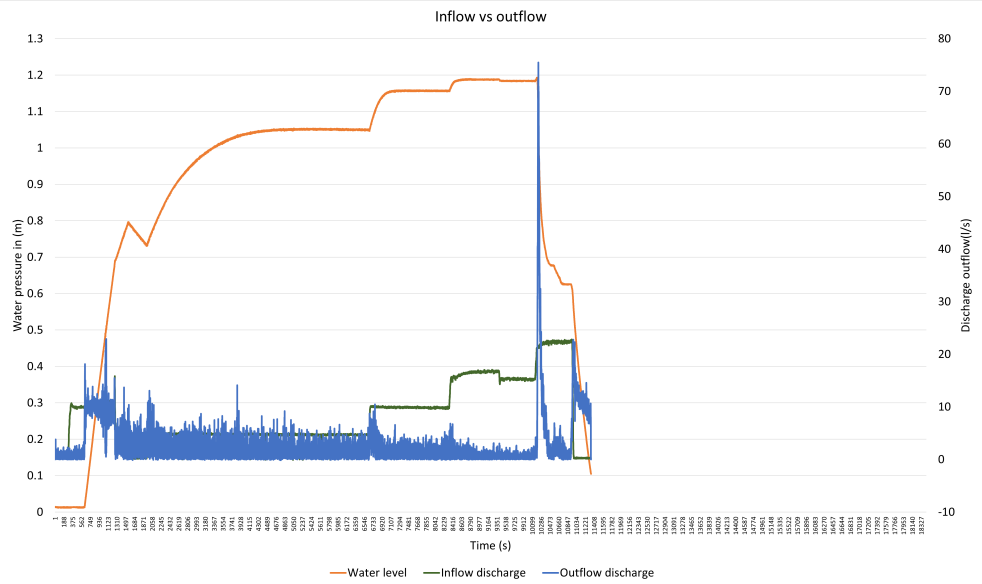

Figure 4.23: Outflow discharge in dumped single layer riprap at dam failure

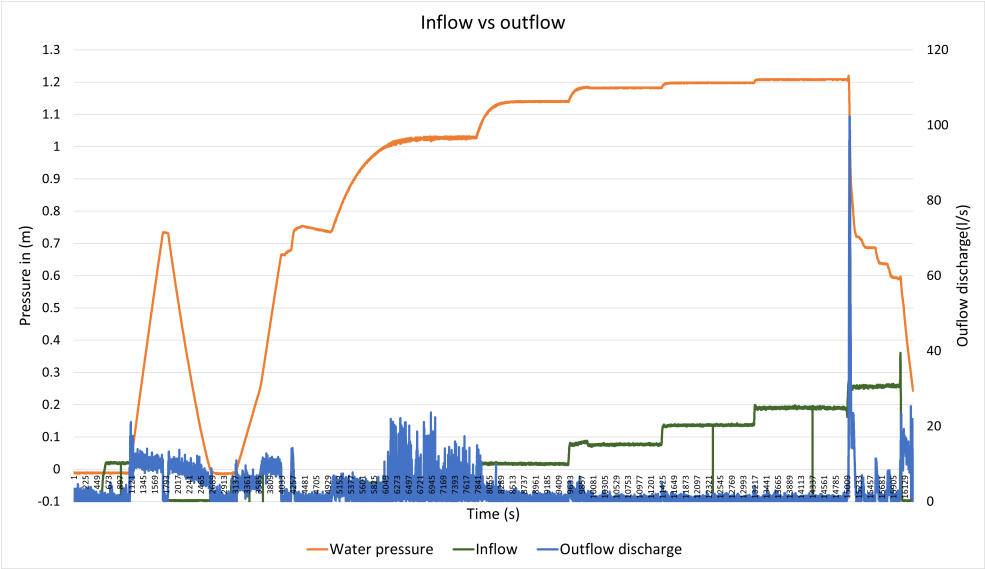

Figure 4.24: Outflow discharge in dumped double layer riprap at dam failure

Chapter 5

Discussion

This section discusses and evaluates the results presented in the results section. Comparison of failure mechanism, breach development rate in placed and dumped riprap, pore water pressure measurements before and after a breach, the velocity of particle calculation using PIV analysis, breach parameters comparison with empirical relation and experimental parameters, and outflow discharge.

5.1 Failure mechanism and process in placed and dumped riprap due to overtopping

In both dumped and placed riprap, the failure started from the just downstream edge of the crest. No aeration was observed on the downstream edge of the crest in dumped riprap, but aeration was observed in placed riprap which is similar to the observation made by Hiller (2017). In both cases, the toe on the downstream side plays a crucial role from the stability point of view which is similar to the Ravindra, Sigtryggsdóttir et al. (2019).

It was observed that in both placed and dumped riprap the overtopping discharge created extra force on the downstream toe of the dam. At a certain point, the toe was not able to take more force from the overtopping discharge, and the developing gap was observed on the downstream edge of the crest. This developing gap was observed due to compaction of riprap material, and exposure of the filter material resulted in the sliding of the riprap on the downstream side. The friction between the dam and ground surface is also an important factor from the stability point of view; in my case, model M2(Dumped single layer riprap) and M3(Placed riprap), the breaching discharge was lower compared to Senarathna (2021) and Ravindra and Sigtryggsdottir (2021) in a similar kind of experiment. It was due to the difference between the geotextile; in their case geotextile was extended up to the filter and riprap; however, in my case, it was only in the shell materials.

In both cases, the dam was filled up to the core level to see the leakage rate; in our case, the leakage was minimum. We noticed that the leakage relates to the

permeability of the core and joint between the core and side edge of the dam. In dumped single-layer riprap, the leakage rate was high than in another riprap it was due to the weak joint between the core and side edge of the dam. The discharge was increased by 5 l/s in both cases to see the precise breaching discharge. We observed that until the breaching discharge has enough energy to erode the riprap material, the model will remain stable.

At specific discharge, the breach starts to occur. It was observed that the breach in placed riprap was more abrupt than in dumped riprap. In placed riprap, if the breach begins, then the breach is continuous; however, in dumped riprap, it was observed that the breach initiates and is stable for a few seconds, and after that, the breaching is continuous. It was also revealed that the breaching discharge and failure time are relatable; the higher the breaching discharge longer will be the breaching time and vice versa refer to figure 4.3, 4.9, 4.11. Placed and dumped layer riprap had higher breaching discharge than single layer riprap, and also they have longer failure time.

5.2 Breach development rate in placed and dumped riprap

To observe the breaching rate, the center position of the crest was taken as a reference point for both placed and dumped riprap. In placed riprap, there was one additional reference point 1 m downstream from the center of the crest, and a comparison of erosion rate was made between them refer to table 4.2 and figure 4.6. It was observed that breach in 1 m d/s lags the erosion rate in the crest. In the period 35 seconds after a breach, the deposition was observed in the 1m downstream section, and in another period, the breach rate was lower compared to the crest. It is due to the steeper slope in the crest compared to the 1 m d/s side.

In both dumped and placed riprap, when the breach started, it was found that the breach rate was very minimal in the beginning. In placed riprap, there was no significant erosion until 25 seconds after breach initiation, and for dumped riprap, it was 10 seconds. In placed riprap, the maximum breach rate was 20 mm/s, and for the single layer and double layer dumped riprap, the maximum breaching rate was 18 mm/s and 30 mm/s, respectively. This highest breaching rate didn't hold for a longer time; with an increase in the period, the breaching rate decreased exponentially, and after a certain period, the stable flow was maintained.

It was found that the breaching rate and peak discharge are relatable higher the peak discharge higher the breaching rate, and vice versa refer to figure 4.13 and 4.6 . In higher breach discharge, it was revealed that more dam materials get eroded than the dam breach with lower discharge.

5.3 Pore water pressure measurements

There are a total of ten pressure sensors for the pressure measurement, nine are inside the dam body, and one is outside the upstream side of the dam. These nine pressure sensors are for the measurement of pressure developed inside the dam and one outside for water head measurement of the incoming flow. Pore water pressure was measured during the whole experiment for all dam models.

In this thesis, only the comparison of pressure measurement just before the breach and just after the breach is done refer to figure 4.14 and 4.15. Before the breach, we can observe that all the pressure lines downstream side of the core are inside the dam. After the breach, the pressure lines are outside the dam due to overtopping action. When the water overtops during breaching, more water is on the downstream side creating higher pressure. Comparing the pore pressure graph, we can observe that there is similar pressure on the upstream side of the core, but on the downstream side of the core, there is a significant change in pressure. From these experiments, it was observed that the pressure development inside the dam doesn't play an important role during the failure due to overtopping; it's due to surface erosion during overtopping.

5.4 PIV Analysis

It's difficult to accurately measure the particle velocity during the high flood and the dam breaching. One way to measure velocity is by taking the video footage during the breach and exporting that video footage in the PIV software. This PIV software will give the velocity of particles during the breaching of the dam.

During the PIV analysis, it was observed that the failure mechanism between two dumped riprap was similar while observation with placed riprap was different this is similar to the Ravindra, Gronz et al. (2020). PIV analysis also found that the breach in placed riprap occurs abruptly, and failure in both dumped and placed riprap starts just downstream section of the dam. It is identical to the failure mechanism finding and process describeds in the above section 4.1.1 and 4.2.1.

In placed riprap, the velocity was observed in the range of 0-0.3 m/s.This first maximum velocity occurred in the first sliding(breach initiation) time and this maximum velocity was also observed at a different time interval. In both single layer and double layer dumped riprap, the velocity was in the range of 0-0.21 m/s. Unlike in placed riprap, the velocities measured at different time intervals were not in the higher range. During the breach, the average velocity in the single-layer was around 0.14 m/s but in the double layer dumped riprap, it was around 0.19m/s.

5.5 Breach Parameters

Different empirical equations were used for the calculation of breach parameters such as breach width, peak discharge, and failure time were determined. These equations are more reliable for the earth-fill dams, and there are few studies carried out on rockfill dams in such empirical equations. In this thesis breach parameter for only dumped riprap is determined from empirical equations. Xu & Zhang (2009) gave a more accurate prediction of breach width than Froehlich, US bureau of reclamation(1988). The peak discharge obtained with these empirical relations is not in range; these equations predicted a much higher peak discharge than the observed peak discharge in the lab during experiments. The failure time obtained from Xu & Zhang (2009) was around two times higher than observed; however, Froehlich(1995a), the US Bureau of Reclammation(1988) gave a much shorter failure time. From this discussion, Xu & Zhang (2009) are more accurate in predicting breach width and failure time in dumped riprap rockfill dams.

5.6 Outflow discharge

It's difficult to measure the outflow discharge directly, so we have used an indirect approach to measure it. Water in the reservoir is related to the height of the water column, and the change in the water column during breach gives the change in water volume in the given period; this means we can determine peak outflow discharge. Peak outflow discharge was observed when there was a sharp fall in pressure for all three dams. On plotting data on the graph refer to figure 4.21, it was found that the peak inflow breach discharge and outflow peak discharge can be related with a linear equation.

5.7 Limitations of Setup

The experiment and test were carried out at NTNU laboratory, and some of the test setups were fixed from the beginning and had limitations such as the size of the flume, pump capacity, reservoir capacity, and other limitations during the construction are core materials, construction methodology, etc. These limitations are briefly described below.

- The flume width is 1 meter, the dam length across the flow was constant for all models when the breach initiates, and after a certain period, the top part of the crest was eroded in all cases. This prevented model from gaining its natural form of breach opening and resulted in a similar type of breach width in all cases. In our study, the breach width was assumed to be symmetrical to the left bank glass side.

- The reservoir size scaling in the upstream side of the dam is small compared to the actual dam, which causes fast draining of reservoir water and leads to a fall in pressure head quickly. This may create a gap in understanding peak outflow discharge, erosion rate, and the relation between inflow and outflow discharge.

- Due to the limitation of the pump set up and reservoir system, the minimum particle size used n the construction of the dam was 0.5mm, which is in the coarser range; this may affect the permeability of the dam. This possibly can affect the phreatic line inside the dam, so for better understanding, it is recommended to use the required size of particles in the dam.

- The rubber membrane was used as a core membrane in the dam, which may not represent the actual permeability of the core. There was a problem with the connection between the dam and glass wall; when more tape was used, the core membrane acted as a single piece of wall, and when less tape was used, more leakage from the edge was observed. It may cause a problem in the understanding of the dam breach event.

- The same material was used for many test experiments. With time the finer material gets eroded and mixed with water causing turbid water; this causes the material to be in the coarser range. The model was prepared manually, transportation of dam material was done by the wheelbarrow, and when dumping with a wheelbarrow, the mix was heterogeneous.

Chapter 6

Concluding Summary and Further Recommendations

This section is about the conclusion made from the experiment carried out on rockfill dam with riprap as erosion protection at NTNU hydraulic lab and further recommendations to better understand the complex nature of the breaching process due to overtopping action in rockfill dams.

6.1 Concluding Summary

Embankment dams are vulnerable to overtopping and excess through flow, as the dam body is mainly constructed with the pervious and erodible material. The initiation of the erosion process may lead to the breaching of the dam. This breaching phenomenon in the dam is a complex process since the breaching process is affected by different factors such as dam material properties, dam type, design, construction methodology, geology, upstream and downstream water levels, and reservoir volume. It is necessary to understand the process and breach opening, estimate the flood in the downstream section, and mapping this for hazard mitigation in the downstream section of the dam. In Norway, most of the embankment dams are earth rockfill dams with erosion protection on the downstream and upstream slope of the crest. The breaching phenomena of such embankment dams have few studies. This thesis added some new information for further understanding the breaching process due to overtopping in rockfill dams with erosion protection.

From the three lab tests of rockfill dams, It is concluded that The dam will not breach for a longer time period even after overtopping; the breach only initiates when the overflow discharge has enough energy to move the riprap materials. In both dumped and placed riprap, the failure starts from the just downstream edge of the crest, and there is aeration in placed riprap on the downstream edge of the crest but not in dumped riprap. The downstream toe plays a crucial role from the stability point of view. During the breach, overtopping discharge creates extra force on the downstream toe of the dam. At a certain point, the toe is not

able to take more force from the overtopping discharge, and the developing gap will be observed on the downstream edge of the crest. This developing gap was observed due to compaction of riprap material, and exposure of the filter material resulted in the sliding of the riprap on the downstream side. It is also found that the higher friction between riprap, and filter material with the ground surface can handle higher breaching discharge and vice versa.

In placed riprap, to calculate the breaching rate crest center and 1m downstream from the crest center and for the dumped riprap crest center was taken for the reference. It was observed that the maximum breaching rate starts after a certain time period of the initial breach, this maximum breach rate only holds for a small time interval, and after that, the breach rate decreases quickly.

In the dam body, there are nine pressure sensors, one in front of the upstream toe to measure the reservoir water level, and nine pressure sensors inside the dam body. On comparing pressure measurements just before and after the dam breach, it was found that all the pressure lines on the downstream side of the core lie inside the dam, and after breaching, these pressure lines lie outside the dam body. It indicates that overtopping will create extra pressure on the downstream side.

From the PIV analysis, it is concluded that the failure between two dumped riprap is similar while observation with placed riprap is different. It was also found that the breach in placed riprap occurs more abruptly than in dumped riprap. During the breach in, placed riprap dam material had a higher velocity than dumped riprap for a similar type of breach conditions; this maximum breach velocity has occurred in the first sliding gap forms (breach initiation) time, and this maximum velocity was also observed at a different time interval; however, in dumped riprap, the breach initiation does not have the highest velocity like placed riprap, and the maximum velocity was observed at a different time interval during the breach.

The breach parameters are calculated with available empirical relations; these relations are more applicable for the earth-fill dam rather than rock-fill dams. However, in this thesis, I have calculated the breach parameters with available equations for dumped riprap. These calculated parameters and observations are highly different. Xu Zhang (2009) gave a more accurate prediction of breach width than Froehlich, US bureau of reclamation(1988).

From the data collected during the experiment, it was found that Peak outflow discharge was observed when there was a sharp fall in pressure for all three dams. Plotting data on the graph showed that the peak inflow breach discharge and outflow peak discharge can be related with a linear equation. It shows that we can predict the outflow discharge during the dam breach and map the flood inundation area on the downstream side to minimize the risk of probable flood during a

dam breach.

6.2 Further Recommendations

There are few studies carried out in the field of failure due to overtopping and breaching of rockfill dams with erosion protection. This thesis has tried to add some bricks in the understanding of overtopping and breaching of rockfill dams with erosion protection. However, there are a number of things that can be improved for a better understanding of the complex nature of dam breaches.

- All rockfill dams were carried out on a fixed slope (1v:1.5H); we can make a different model with a different slope so that we can have a better understanding of the breaching of dams on different slopes.

- The dam width, reservoir capacity can be increased to a bigger size with a different model setup and a number of pieces of rubber membrane connected with light tape to use as a core membrane instead of a single membrane tape to see the natural breaching event.

- It needs to be carried out in large-scale field tests of rockfill dam to better understand the failure mechanism and minimize the scaling effects.

- The friction on the toe is crucial from the stability point of view; the site and model should have a similar friction coefficient between riprap and ground surface.

- It is recommended to use a mechanical sieving system for the separation of filter material and shell material after a dam breach; manual separation causes more heterogeneous material during the construction of the dam.

- The velocity of the particle during the breach of the dam was determined with the help of FUDAA PIV software; we can add acceleration and the gyroscope measurements in some stones to compare the results from software and test measurements.

- This lab test can be integrated with numerical modeling, and then we will have the flexibility to change the different physical parameters such as discharge, the thickness of filter material, riprap size and thickness, etc., to see the change in results. It minimizes the difficulties of seeing results with a physical model.

Bibliography

Abt, G., Thornton & Ullaman. (2008). Ound-shaped riprap stabilization in overtopping flow. *ydraul. Eng*, *134*.

Bunte. (2001). *Sampling surface and subsurface particle-size distributions in wadable gravel- and cobble-bed streams for analyses in sediment transport , hydraulics , and streambed monitoring*.

Fell, R., MacGregor, P., Stapledon, D. & Bell, G. (2005). *Geotechnical engineering of dams*. A. A. Balkema Publishers Leiden, Netherlands.

Froehlich, D. C. (1995a). Embankment dam breach parameters revisited. *Proc. Conference on Water Resources Engineering, San Antonio, Texas, 1995*.

Froehlich, D. C. (1995b). Peak outflow from breached embankment dam. *Journal of water Resources Planning and management*, *121*(1), 90–97.

Fujita. (1998). Large-scale particle image velocimetry for discharge analysis in hydraulic engineering applications. *Journal of Hydraulic Research*, *36*, 397–414.

Hiller, P. H. (2017). *Riprap design on the downstream slopes of rockfill dams* (Doctoral dissertation). Norwegian University of Science and Technology.

ICOLD. (2011). *Definition of a large dam*. International Commission on Large Dams. https://www.icold-cigb.org/GB/dams/definition_of_a_large_dam.asp

ICOLD. (2022). *Role of dams*. International Commission on Large Dams. https://www.icold-cigb.org/GB/dams/definition_of_a_large_dam.asp

Kjærnsli, B., Valstad, T. & Høeg, K. (1992). Rockfill dams. design and construction. *Hydropower Development*, *No. 10*.

Morris, M. (2009). Breaching processes: A state of the art review.

Muste M, F. I. (2008). Large-scale particle image velocimetry for measurements in riverine environments. *Water Resources Research*.

Nord G, L., Esteves. (2009). Effect of particle density and in discharge concentration of suspended sediment on bed load transport in rill discharge. *Earth Surface Processes and Land forms*, *34*, 253–263.

NVE. (2012). *Veileder for fyllingsdammer*. In: ENERGIDIREKTORAT, N. V.-O.

Olivier, H. (1967). Through and overflow rockfill dams-new design techniques.(includes appendices). *Proceedings of the Institution of Civil Engineers*, *36*(3), 433–471.

Pfister, M. & Chanson, H. (2012). Discussion to scale effects in physical hydraulic engineering models. *Journal of Hydraulic Research*, *50*(ARTICLE), 244–246.

Ravindra, G. (2018). *Hydraulic and structural evaluation of rockfill dam behavior when exposed to throughflow and overtopping scenarios* (Doctoral dissertation). Norwegian University of Science and Technology.

Ravindra, G., Gronz, O., Dost, B. & Sigtryggsdottir, F. G. (2020). Description of failure mechanism in placed riprap on steep slope with unsupported toe using smartstone probes.

Ravindra, G. & Sigtryggsdottir, F. G. (2021). *Rockfill dams – downstream riprap and dam toe*. Norwegian Water Resources and Energy.

Ravindra, G., Sigtryggsdóttir, F. G., Asbølmo, M. & Lia, L. (2019). Toe support conditions for placed ripraps on rockfill dams - a field survey. *VANN*, (3).

Senarathna, N. (2021). Effect of downstream erosion protection on the breaching of rockfill dams.

Siebel, R. (2007). Experimental investigations on the stability of riprap layers on overtoppable earthdams. https://doi.org/10.1007/s10652-007-9041-8

Singh, V. & Scarlatos, P. (1989). Breach erosion of earth-fill dams and flood routing(beed) model,environmental laboratory,us army corps of engineers.

U.S.Bureau, o. R. (1988). *Downstream hazard classification guidelines*. US Department of the Interior, Bureau of Reclamation.

Walder, J. & O'Connor, J. (1997). Methods for predicting peak discharge caused by failure of natural or constructed earthen dams. *Water Resources Research*, *33*, 2337–2348.

Walder, J. & O'Connor, J. (2018). *Fudaa-lspiv version 1.6.4 user manual*.

Xu, Y. & Zhang, L. M. (2009). Breaching parameters for earth and rockfill dams. *Geotech. Geoenviron. Eng., 2009, 135(12): 1957-1970*.

Zhenming, S., Gongding, Z., Ming, P., Qingzhao, Z., Yuanyuan, Z. & Mingjun, Z. (2022). Experimental investigation on the breaching process of landslide dams with differing materials under different inflow conditions, 9–11.

Appendix A

Pore pressure and Inflow Discharge

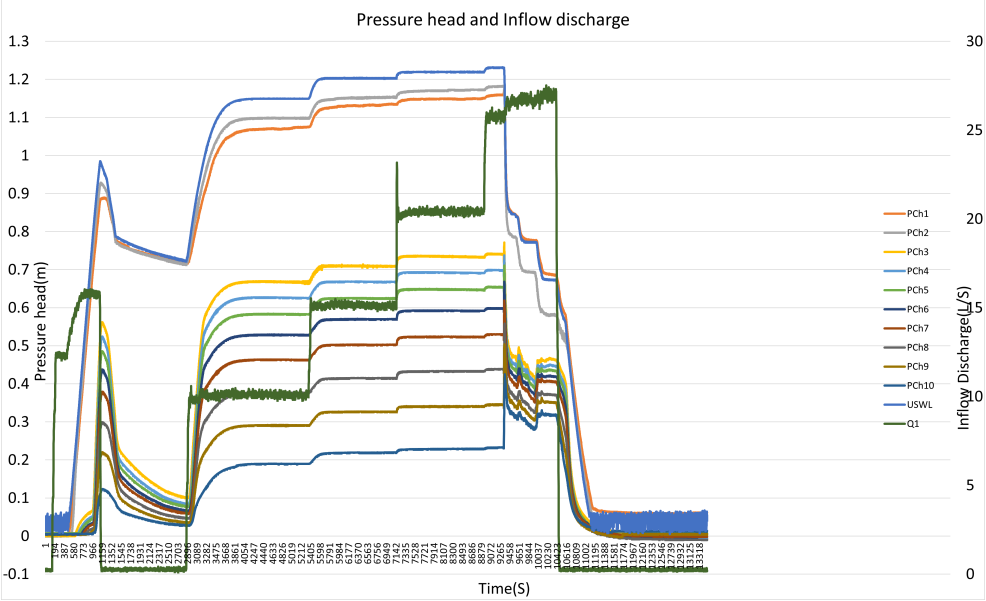

Figure A.1: Pore pressure and Inflow discharge of Placed riprap during the experiment

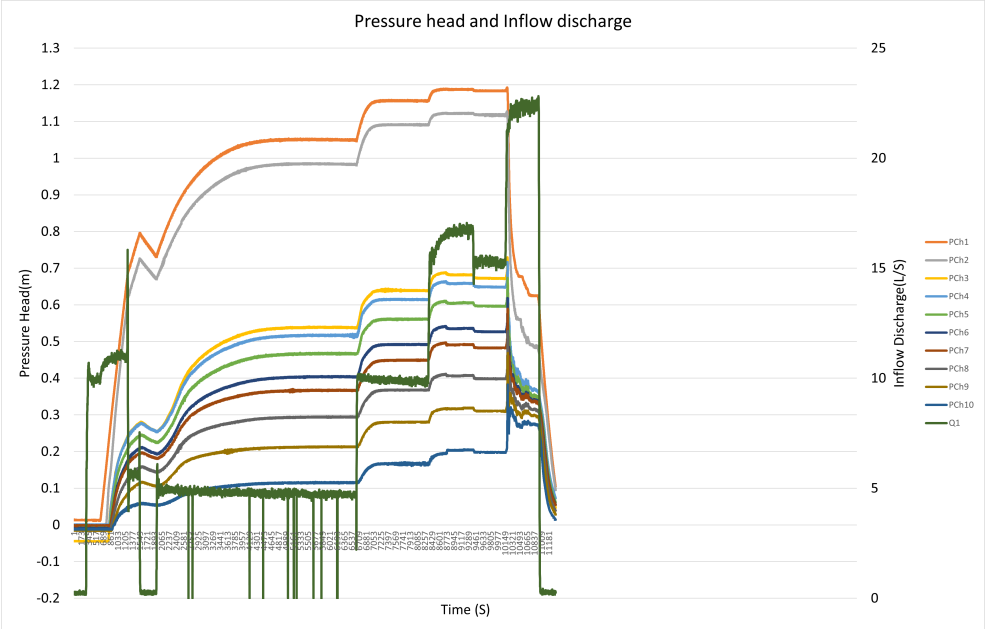

Figure A.2: Pore pressure and Inflow discharge of Single layer dumped riprap during the experiment

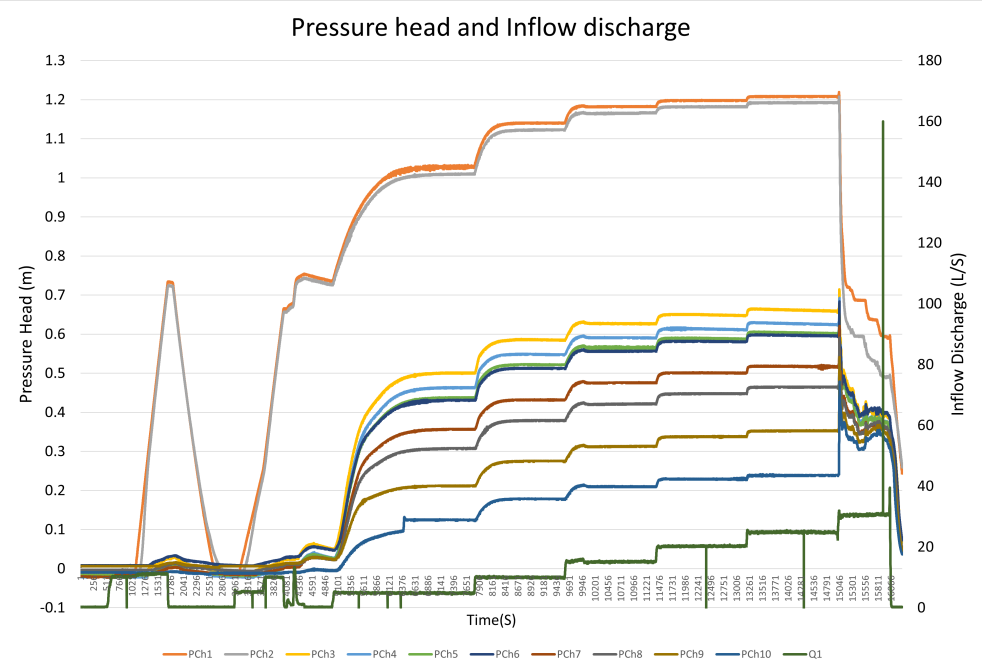

Figure A.3: Pore pressure and Inflow discharge of double layer dumped riprap during the experiment

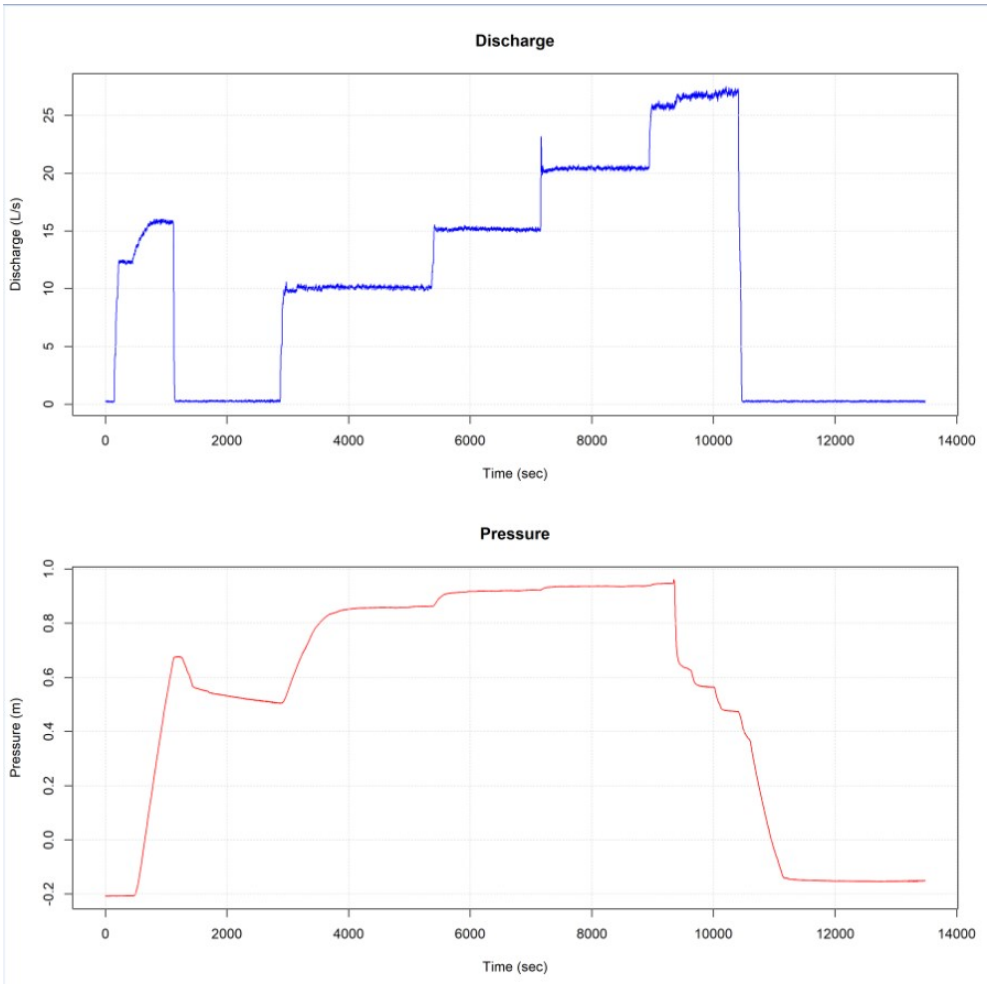

Figure A.4: Inflow discharge and reservoir water level Placed riprap

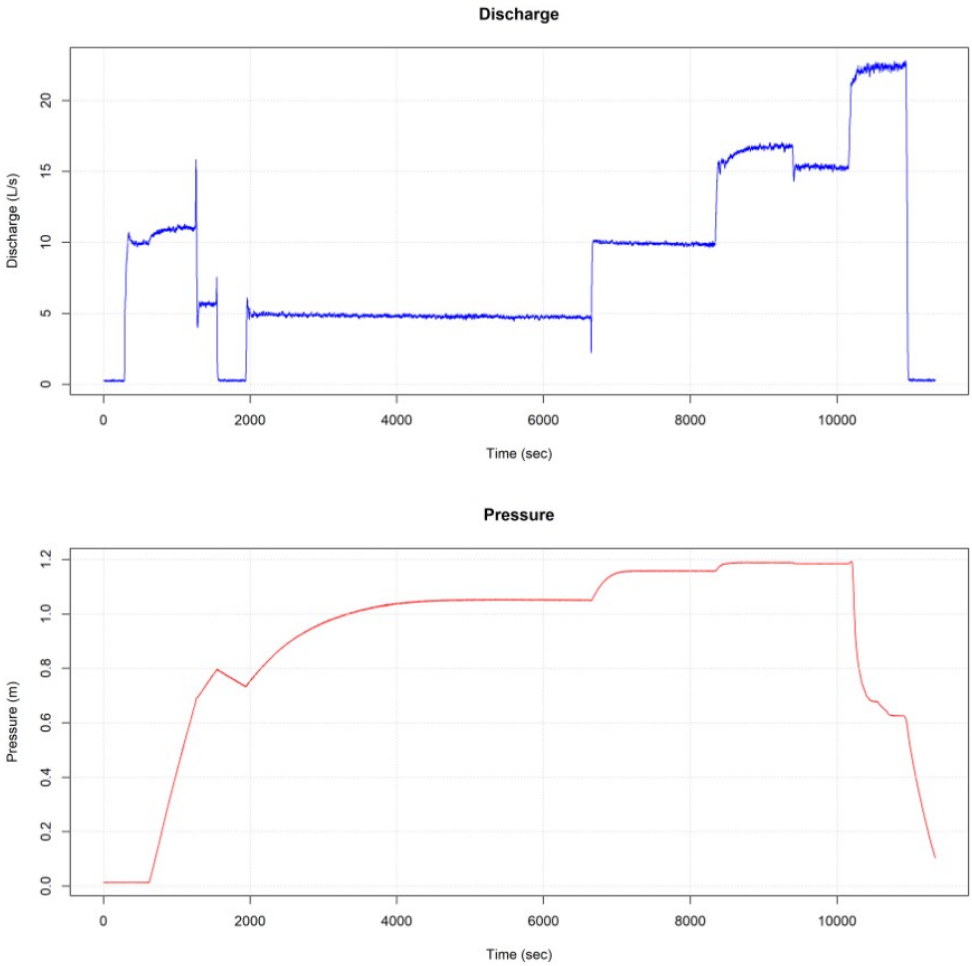

Figure A.5: Inflow discharge and reservoir water level single layer dumped riprap

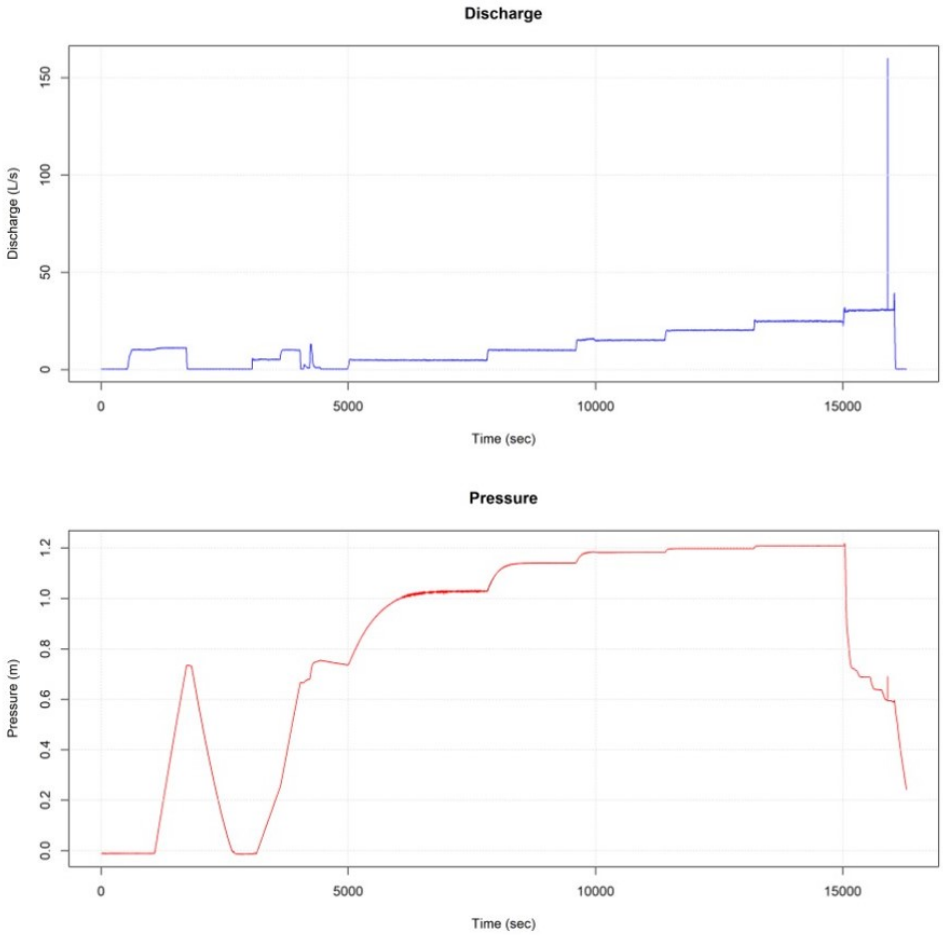

Figure A.6: Inflow discharge and reservoir water level double layer dumped riprap

Appendix B

Data of Manual Breach Measurements

Table B.1: Manual Breach Measurements in Placed riprap

Chainage(cm)	Cross section(cm)				
	-100	-50	0	50	100
0	0.435	0.512	0.572	0.603	0.6
25	0.457	0.517	0.58	0.582	0.548
50	0.473	0.513	0.505	0.547	0.579
75	0.395	0.247	0.39	0.545	0.602
100	0.268	0.263	0.3	0.477	0.598

Table B.2: Manual Breach Measurements in Single layer dumped riprap

Chainage(cm)	Cross section(cm)				
	-100	-50	0	50	100
0	32.4	49.8	64.8	69.7	69.4
25	41.2	57.9	54.7	68.3	71.3
50	53.7	55.5	42.6	58.2	62.7
75	49	31.8	30	45.6	48.3
100	29.8	23	3.5	12.5	31.2

Table B.3: Manual Breach Measurements in double layer dumped riprap

Chainage(cm)	Cross section(cm)				
	-100	-50	0	50	100
0	58.2	61.8	66.3	73.5	69.3
25	57.9	59.5	59.5	70.2	68.5
50	50.8	46.9	51.8	61.1	63.1
75	43.5	33.5	40.5	48.7	62.3
100	37.2	30.2	37.2	55.6	60

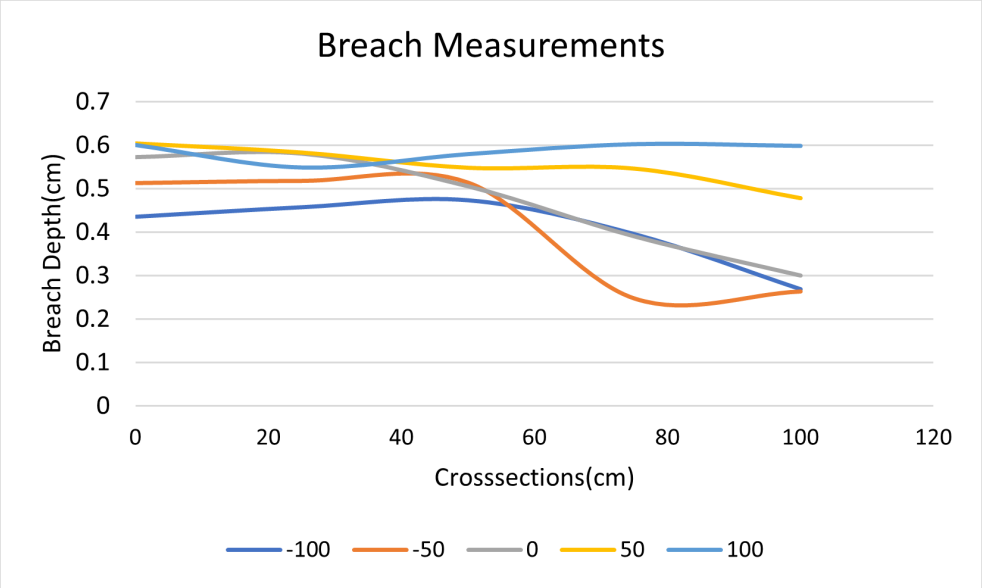

Figure B.1: Manual Breach Measurements in Placed riprap

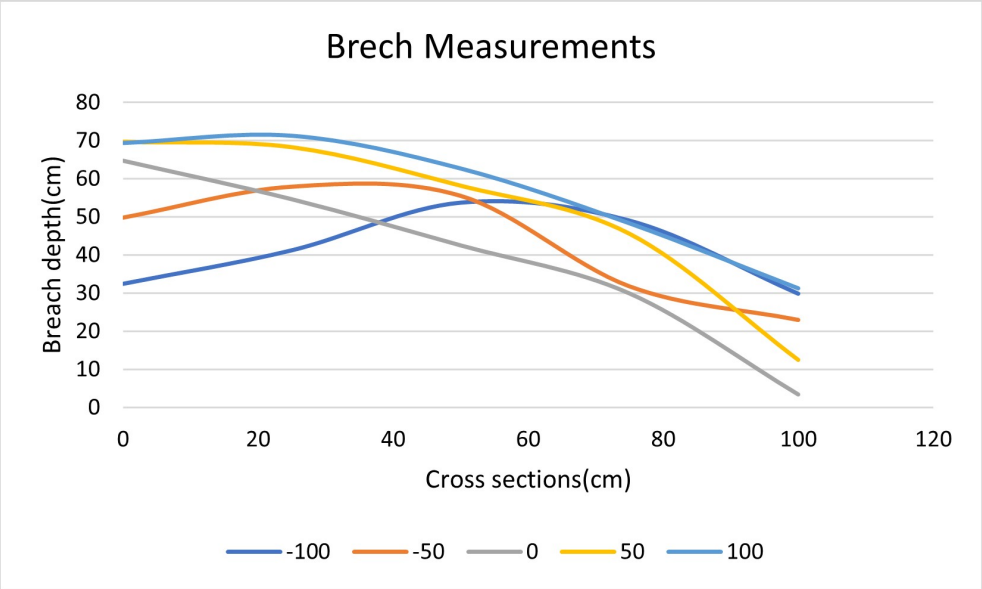

Figure B.2: Manual Breach Measurements in single layer dumped riprap

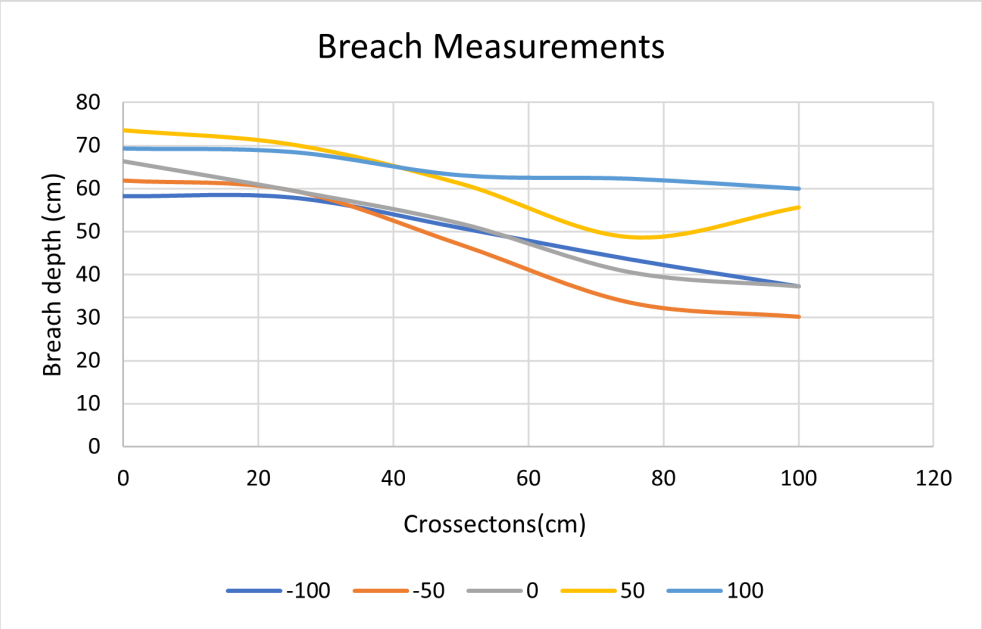

Figure B.3: Manual Breach Measurements in double layer dumped riprap

Appendix C

PIV Analysis Images

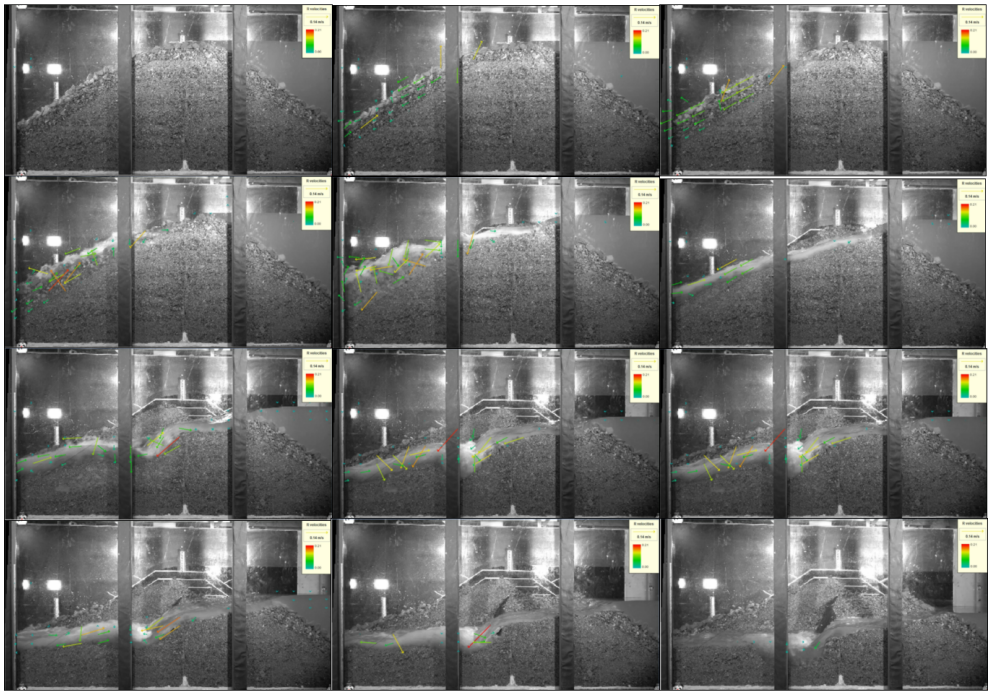

Figure C.1: Particle image velcoity at different time step of single layer dumped riprap

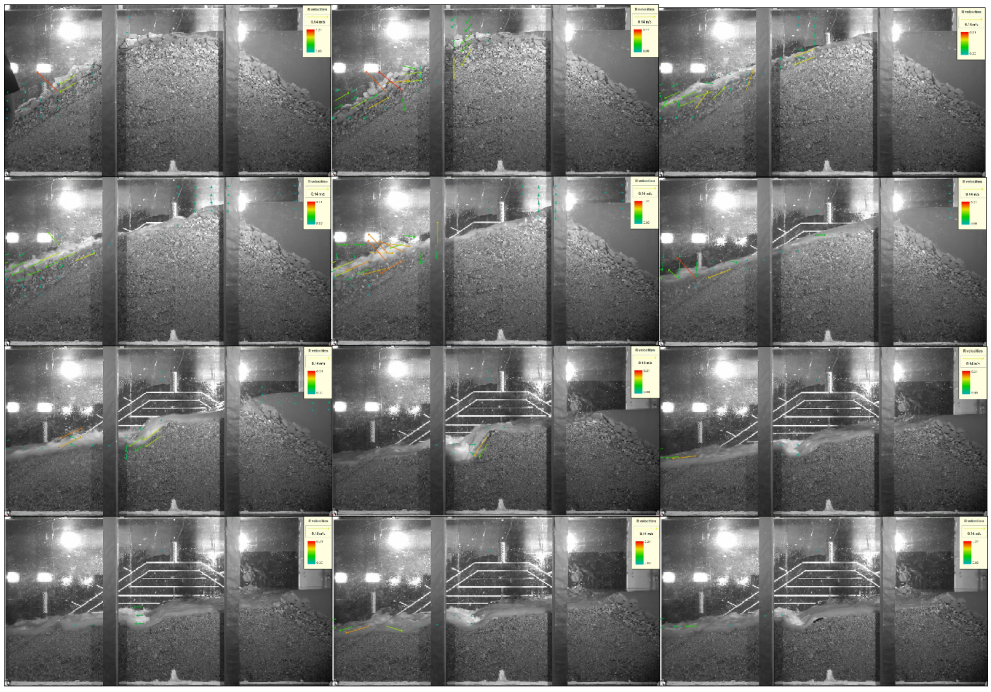

Figure C.2: Particle image velcoity at different time step of double layer dumped riprap

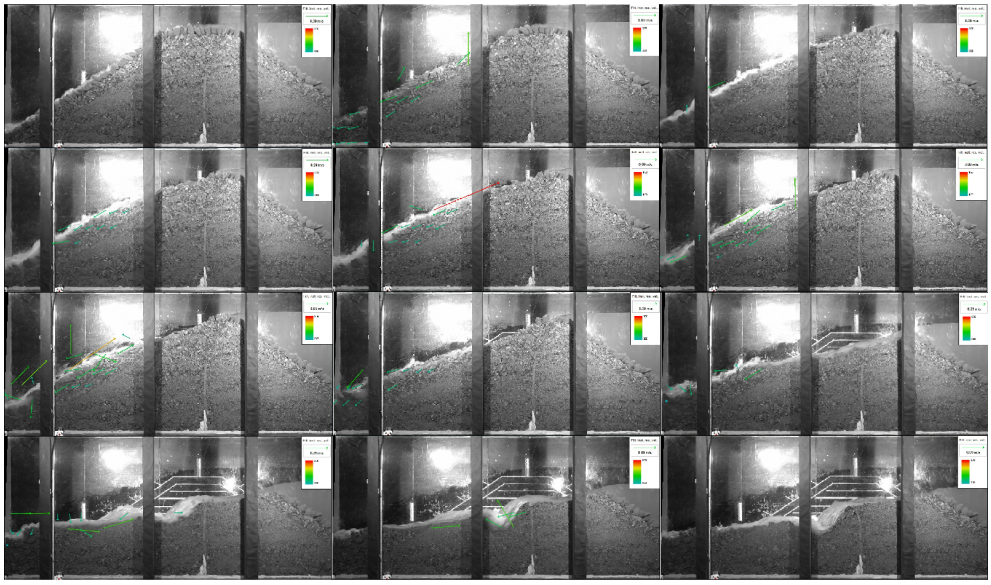

Figure C.3: Particle image velcoity at different time step of Placed riprap

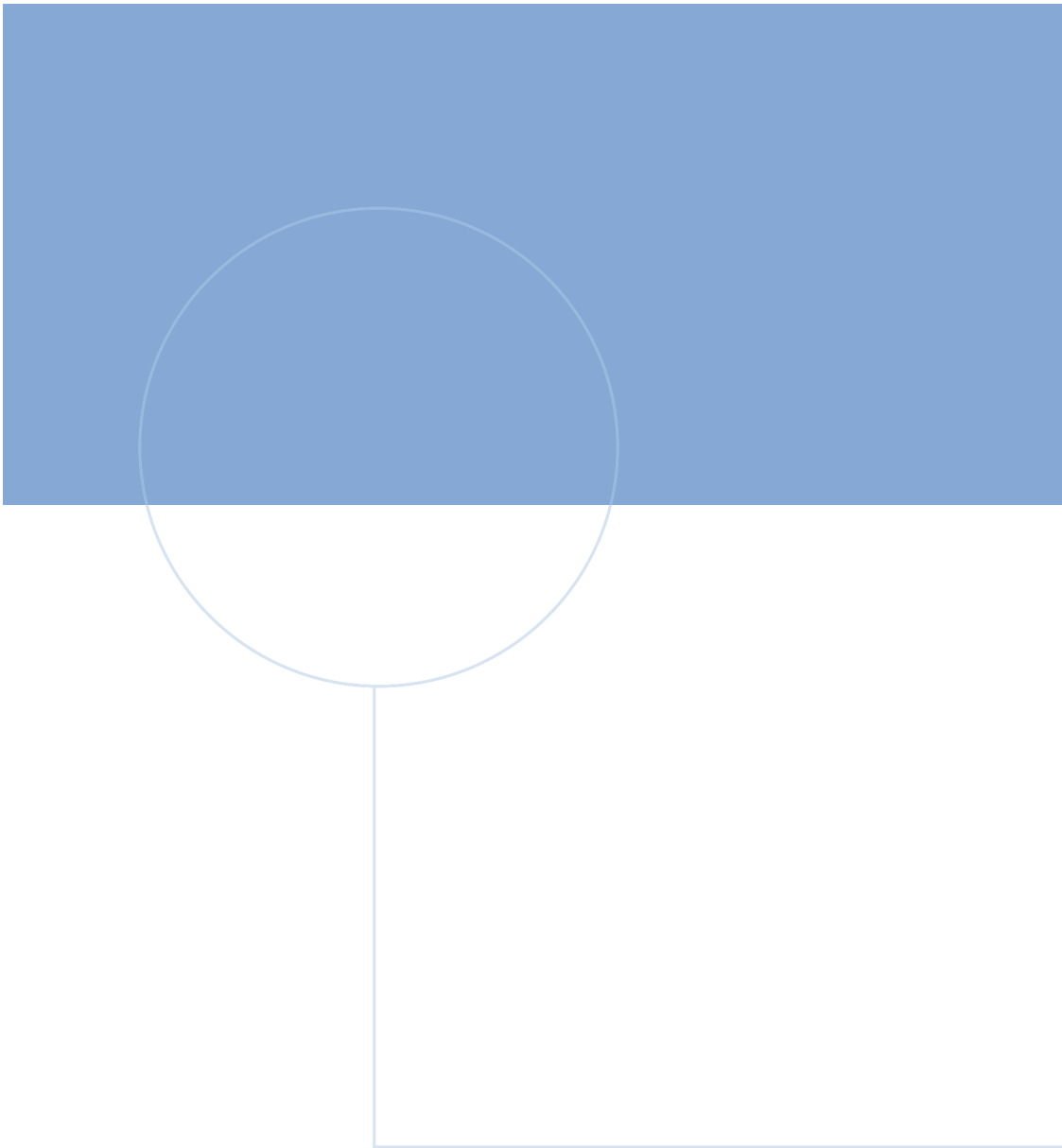

NTNU

Kunnskap for en bedre verden